2009 4 2

牛顿力学 量子力学

费米波长

宏观 ⟷ 纳米

特征尺寸

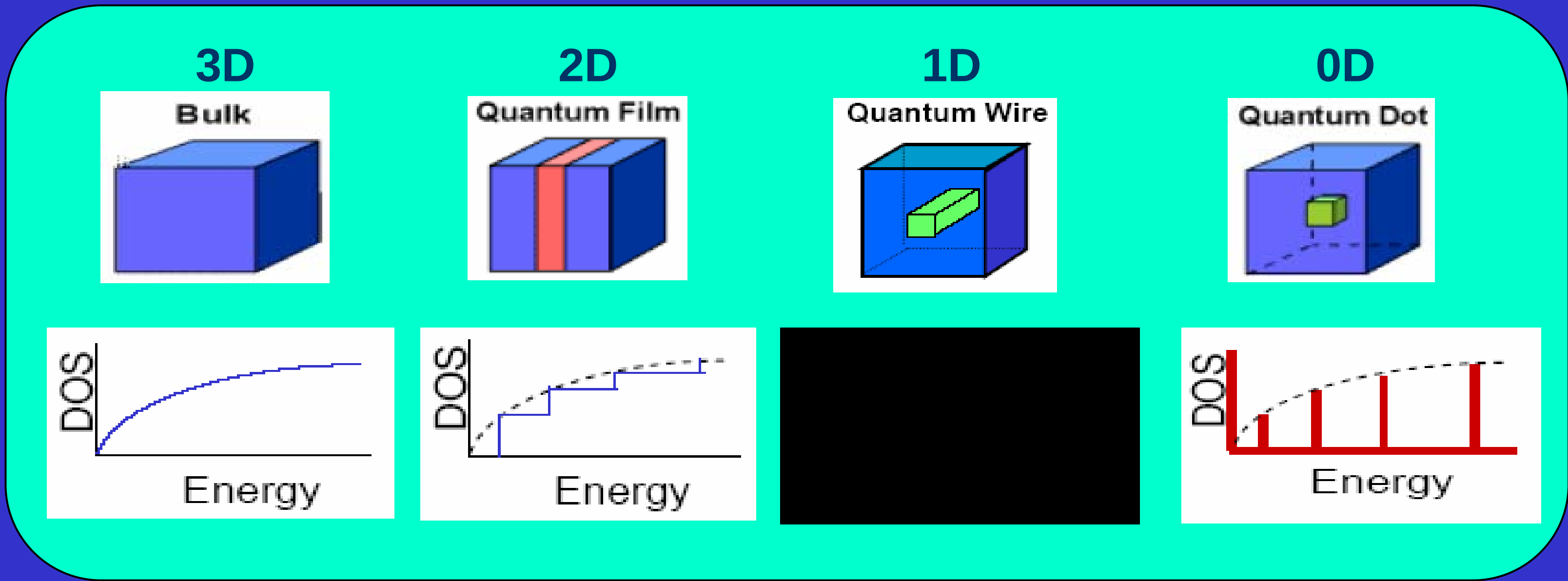

- < 1nm :
  nm
  —
  100nm
- (Coulomb Blockade)
  (Ballistic Transport)
-
-

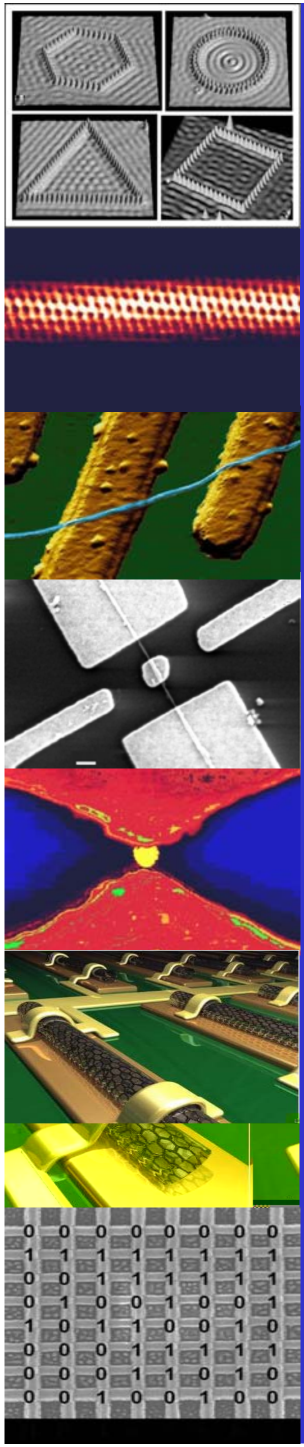

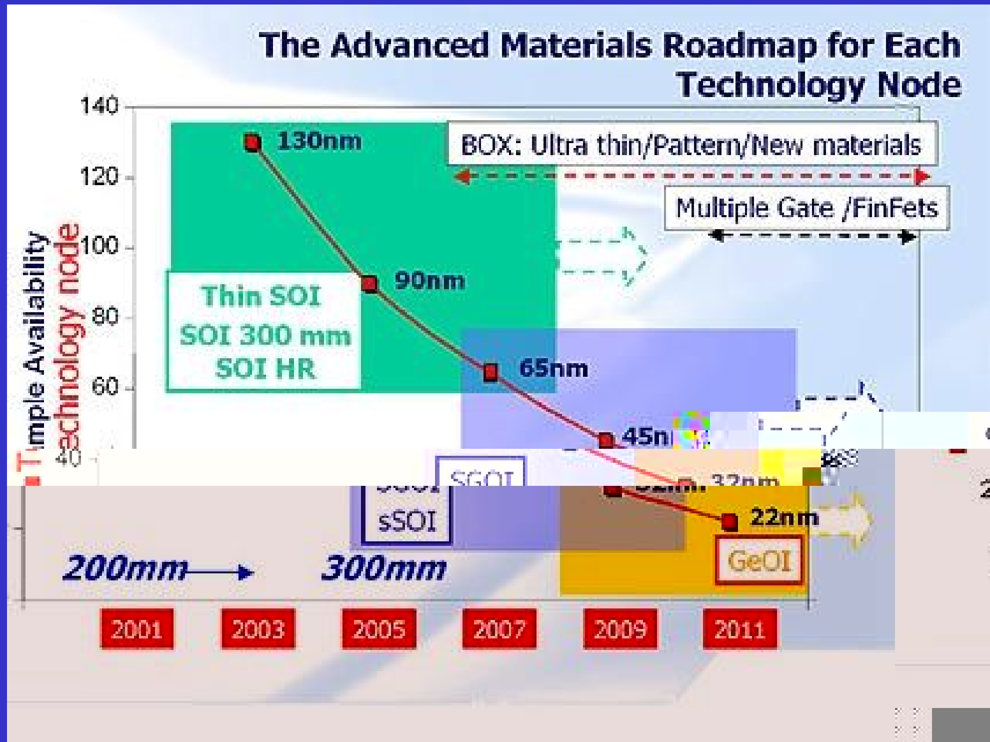

The Advanced Materials Roadmap for Each Technology Node
140
120
100
80
60
40
Timple Availability
Technology node
130nm
90nm
65nm
45nm
32nm
22nm
BOX: Ultra thin/Pattern/New materials
Multiple Gate /FinFets
Thin SOI
SOI 300 mm
SOI HR
SGOI
sSOI
GeOI
200mm
300mm
2001
2003
2005
2007
2009
2011

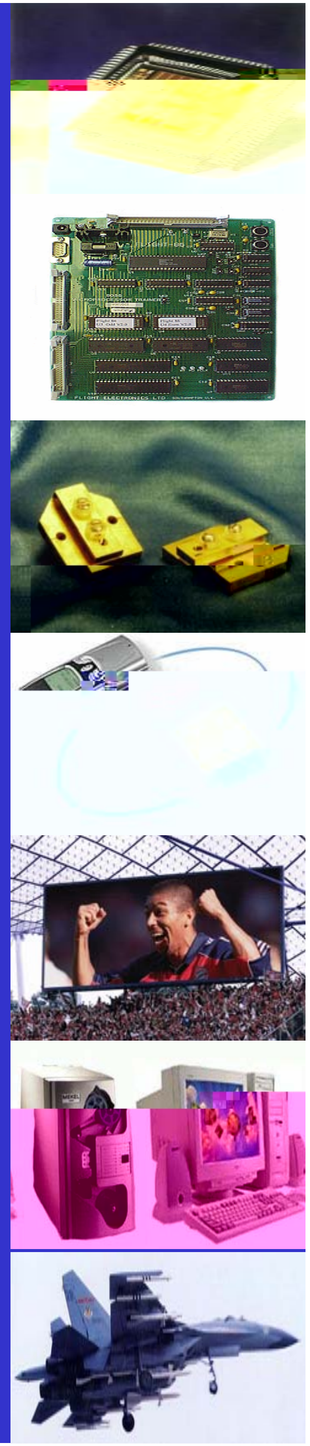

- How to control the identity, placement, and function of every important atom in a nanoscale solid
- How to understand the systems that are too large to be handled by bruteforce calculation, but too small to be tackled by statistical methods?

A frontier science —— a mature discipline

- A revolutionary impact on fields from materials to information, and from energy to biology.

Fabrication of magnetic nanostructures

- **“Top Down”**

  well controlled in several tens nanometer

- **“Bottom up”**

  an art rather than a technology

- /

- :

- X
- STM AFM
-

Laboratory of Microfabrication

Photolithography

MA6 mask aligner

- resolution: < 0.5µm
  @vacuum contact
- mask size: up to 6”
- substrate size: up to 6”
- alignment: two-side
  infrared

Overview of Align/Expose/Develop Steps

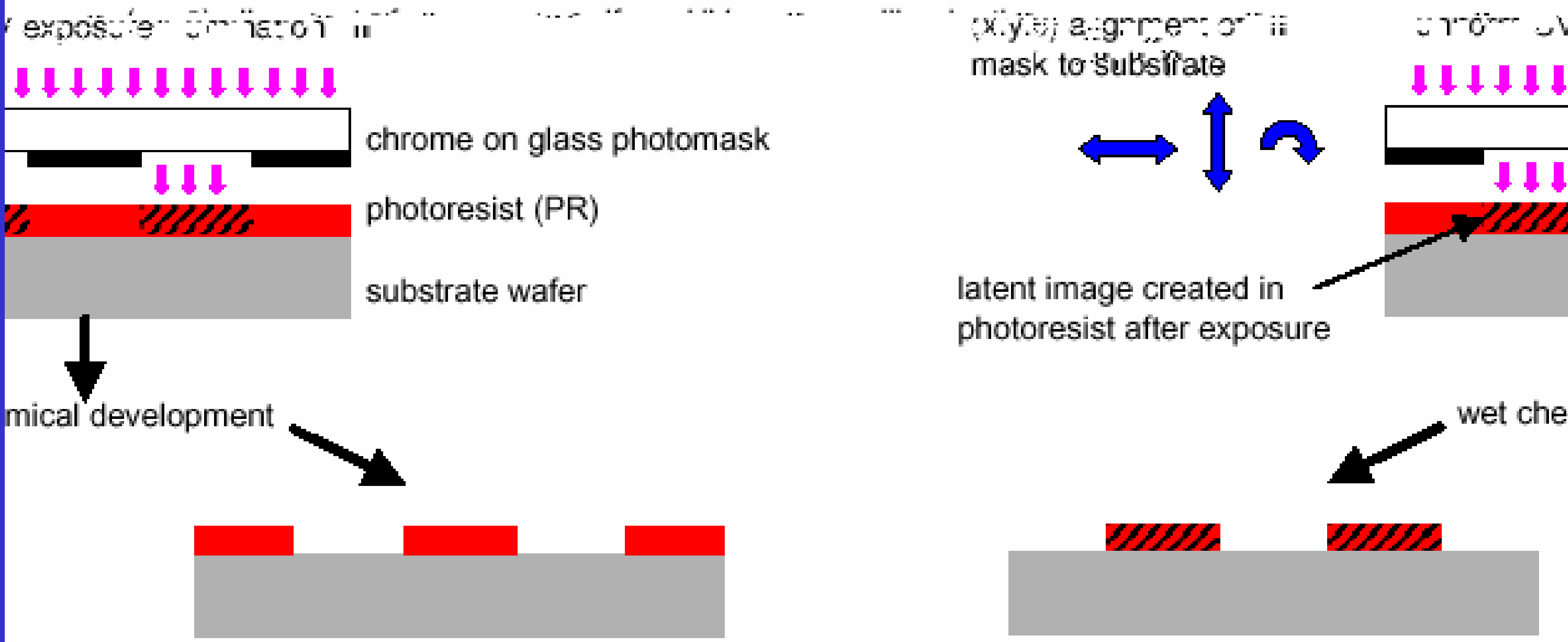

POSITIVE PHOTORESIST

Exposure decomposes a development inhibitor and developer solution only dissolves photoresist in the exposed areas.

NEGATIVE PHOTORESIST

Photoresist is photopolymerized where exposed and rendered insoluble to the developer solution.

Typical Results of MA6

Resolution: < 0.5 micrometer

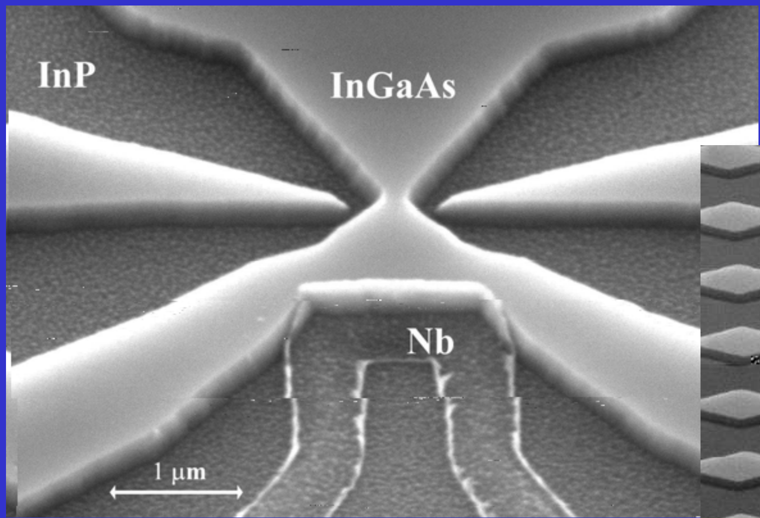

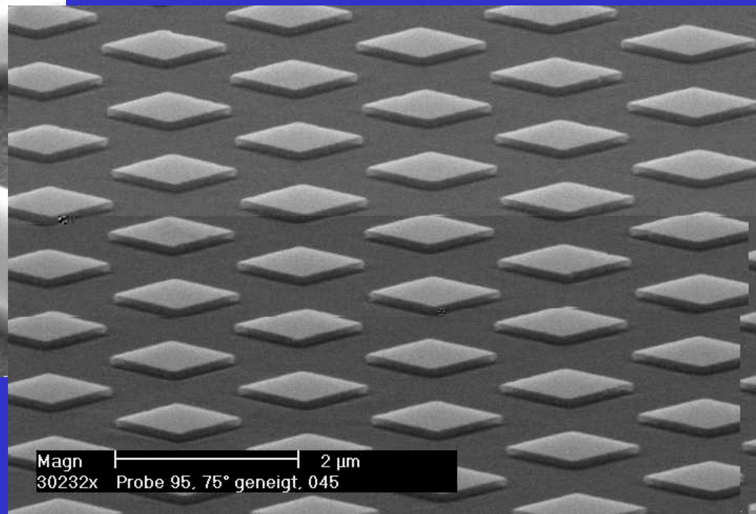

$R=k\cdot \lambda /NA$

Electron Beam Lithography

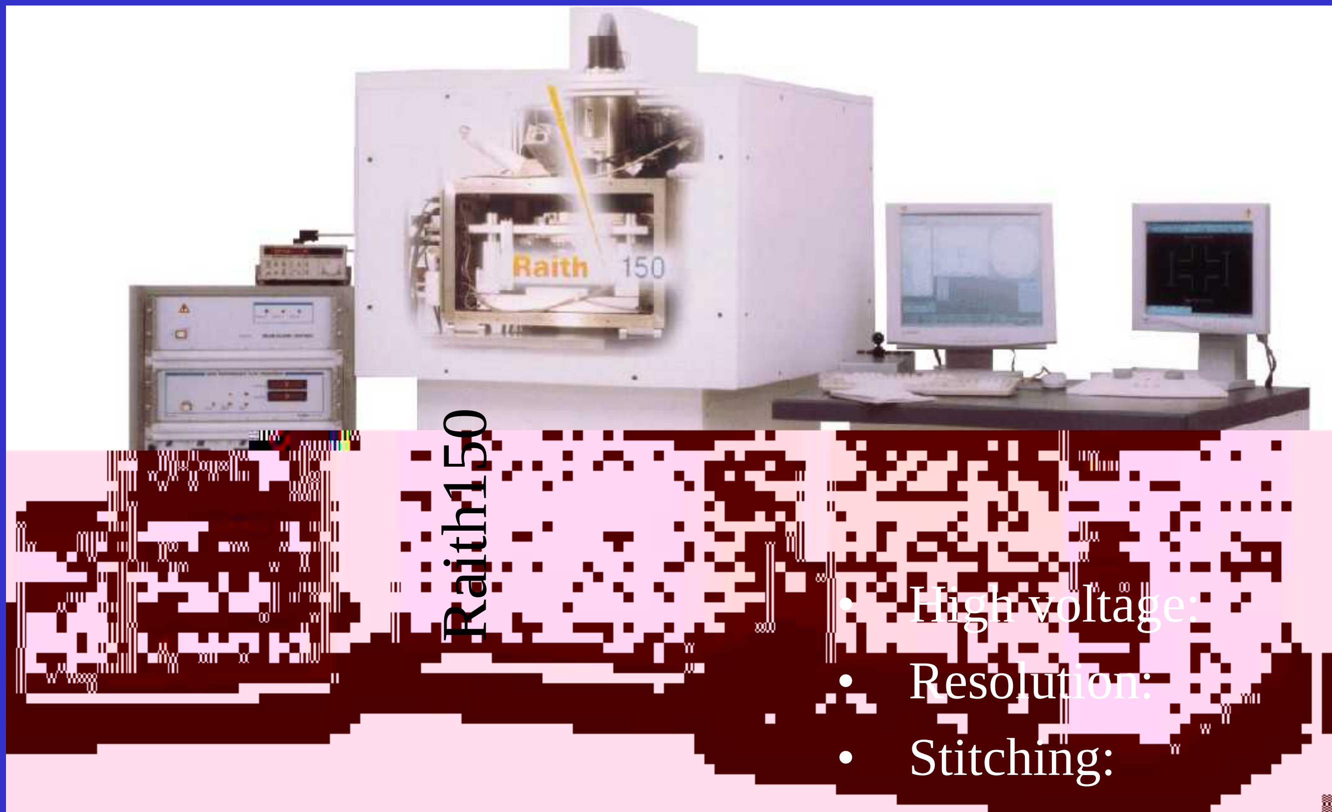

- High voltage: 0.2kV~30kV
- Resolution: 50 nm
- Stitching: 20 nm
- Overlay: 20 nm

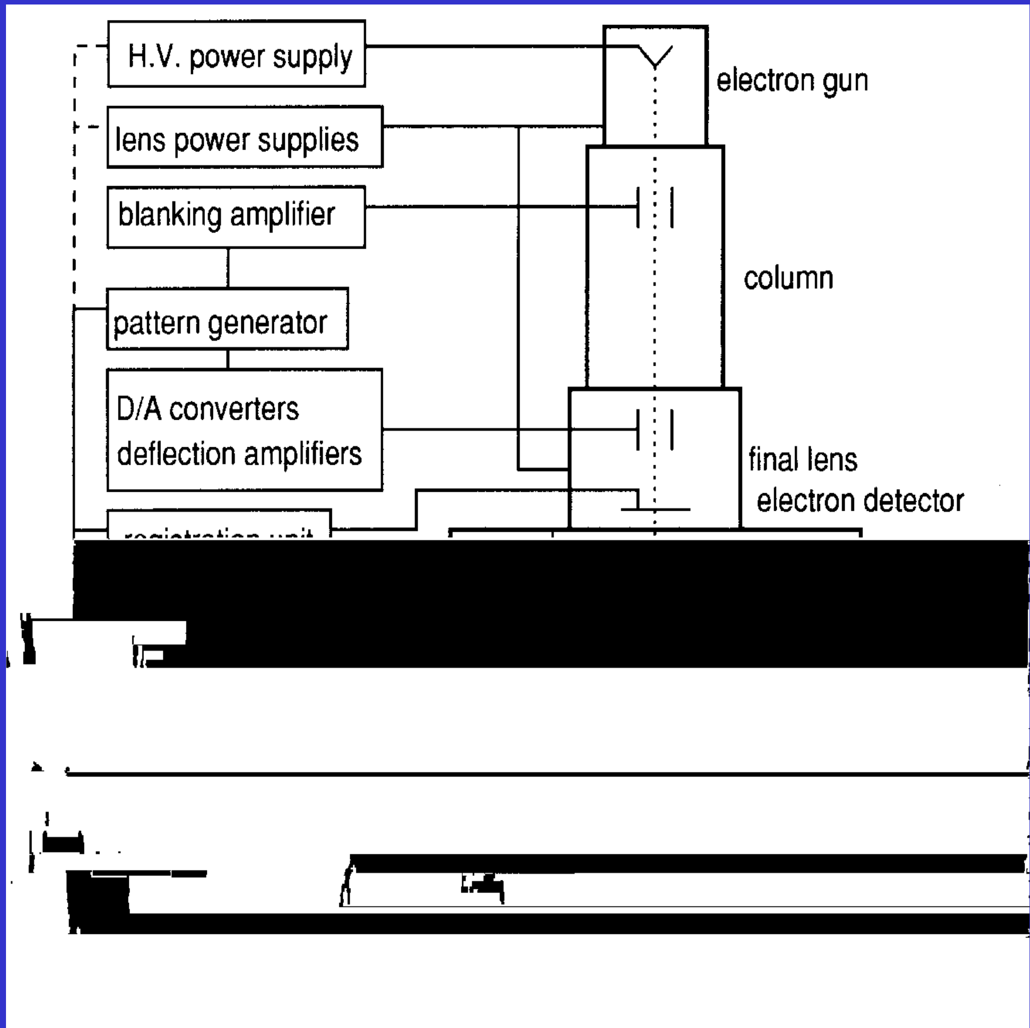

:

$$L = 1.2/(V_b)^{1/2}\ nm$$

25kV

0.008 nm

Focused Ion Beam Lithography

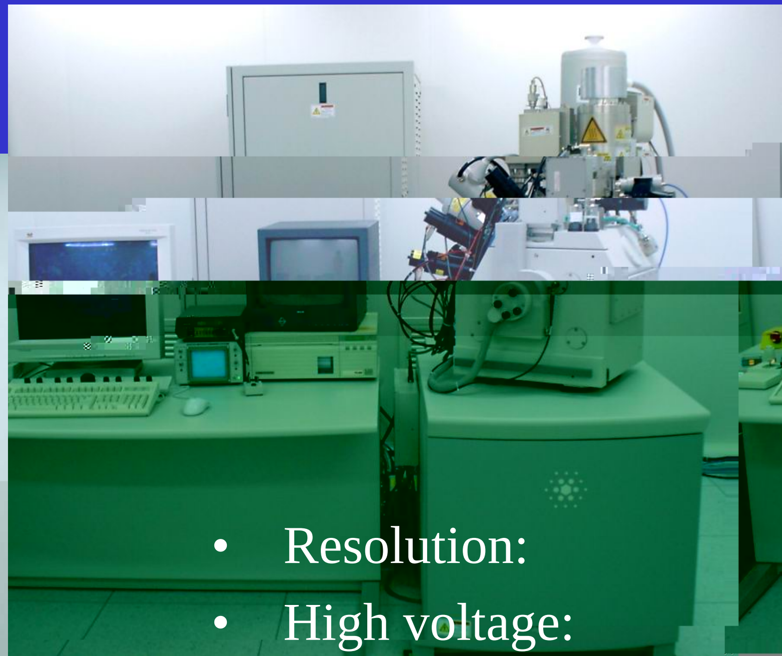

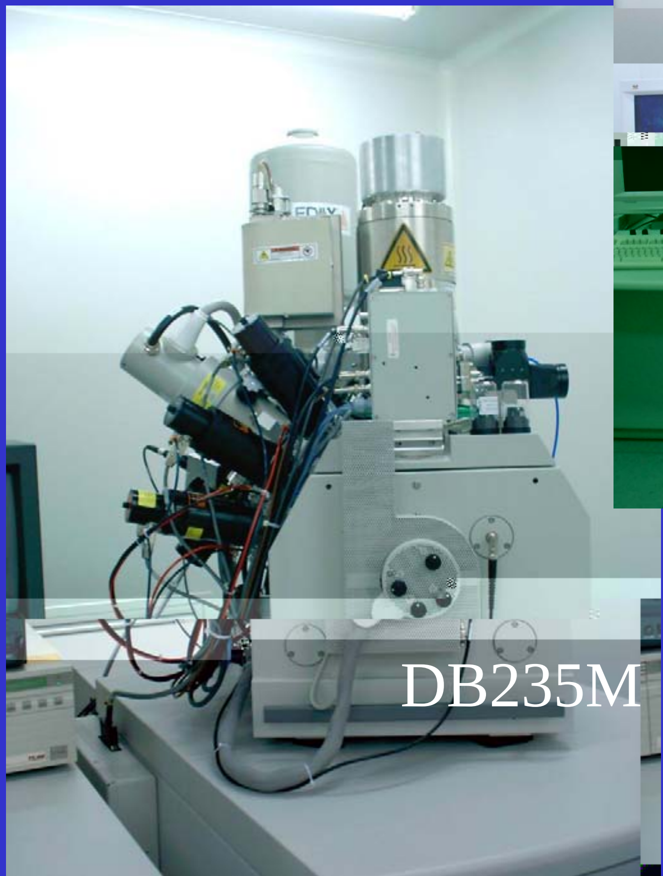

DB235M

- Resolution: 5 nm
- High voltage: 8kV~30kV
- Motorized stage: 6 axes
- Function: etching, deposition

Typical Results of FIB

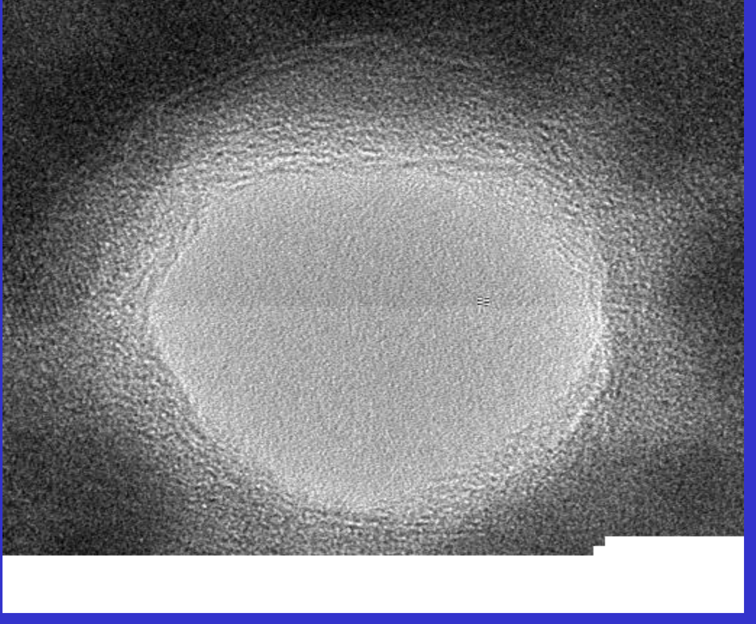

Ion beam resolution: 5 nm

The minimum line width: 10 nm

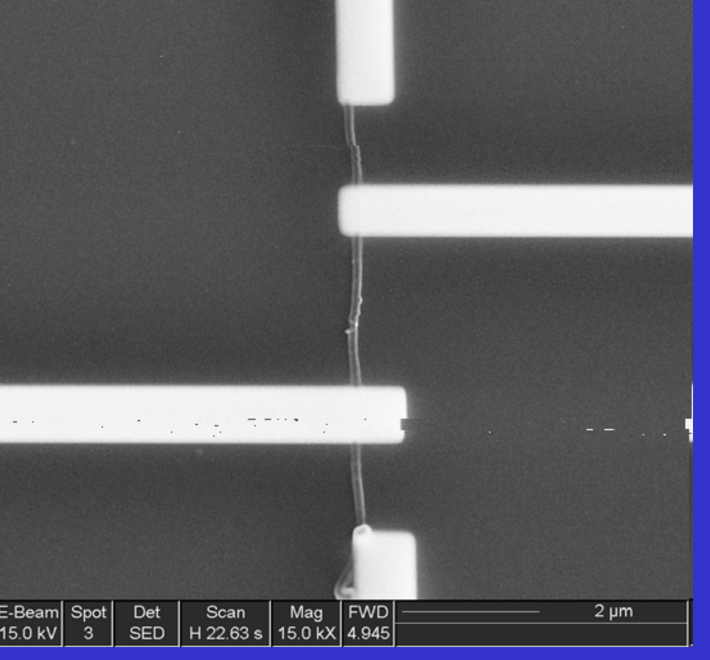

FIB/SEM

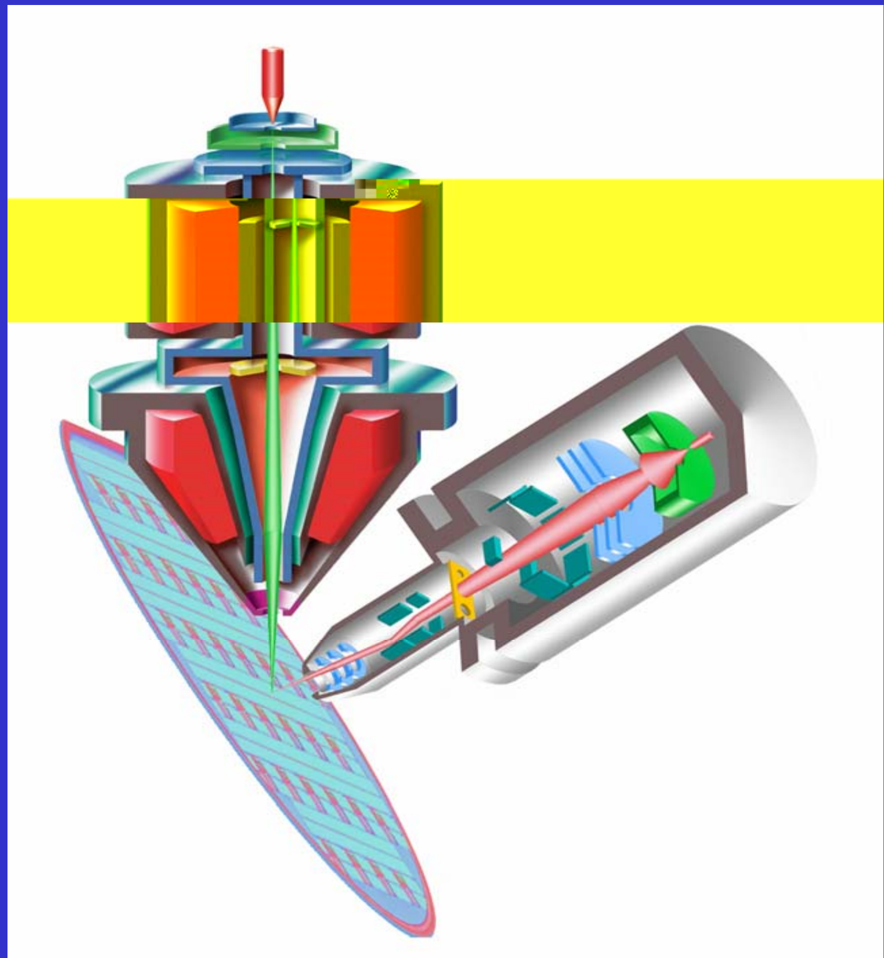

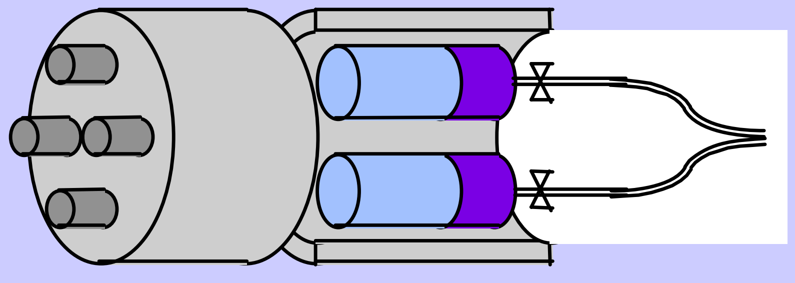

Operating Principle of FIB

1. Ion-solid interaction

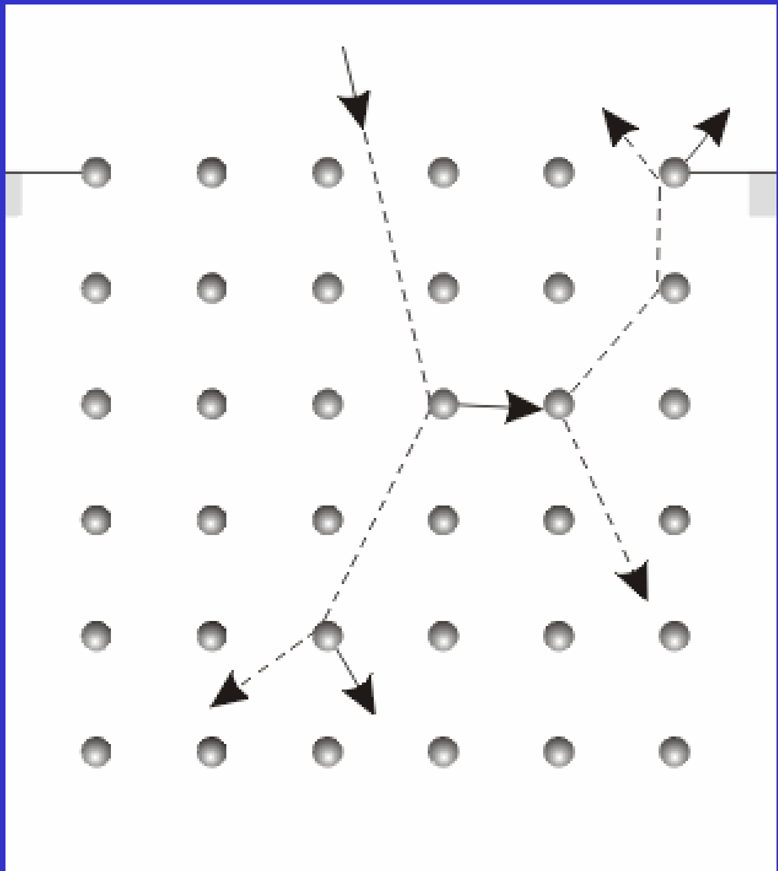

The primary ion produces a linear collision cascade, in which almost only binary collisions occur. Due to this cascade, energy can be transferred back to the surface. If more energy than the surface-binding-energy is placed upon a surface atom, it can be removed from the sample. The average number of atoms removed by one primary ion is called sputter yield (Y). It is strongly depended on the material, ion energy, incidence angle and environmental conditions.

2. Basics of beam deposition (Pt)

A heated capillary is used to inject a precursor gas eg. $Pt(CO)_6$ (Platinum-hexacarbonyl) nearby the beam. Due to the particle beam (either electrons or ions) energy is deposited onto the precursor molecule. The molecule decomposes and the metal atom is bound to the surface.

The applications of FIB

- cross-sectional imaging through semiconductor devices (or any layered structure)
- modification of the electrical routing on semiconductor devices
- failure analysis
- mask repair
- preparation for physical-chemical analysis
- preparation of specimens for transmission electron microscopy (TEM)
- Micro/nano-machining

Local cut and connection

- **Device modification (2 cuts and 1 metal deposition)**

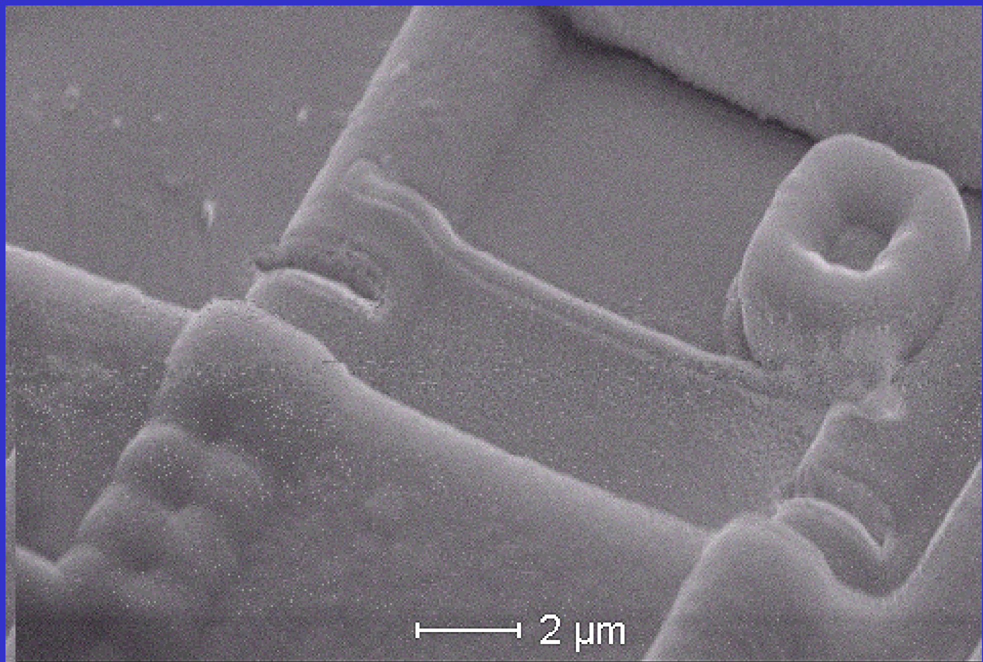

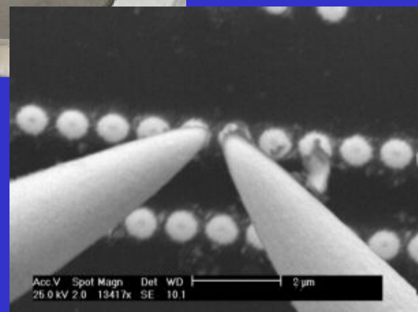

Sample preparation

1 Cross-section for failure analysis and design assistance

2 TEM sample preparation

- Cross-section of an integrated circuit

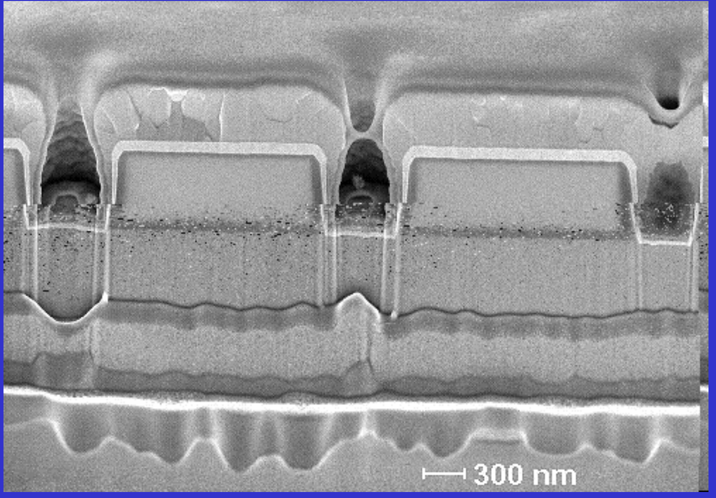

- TEM sample preparation

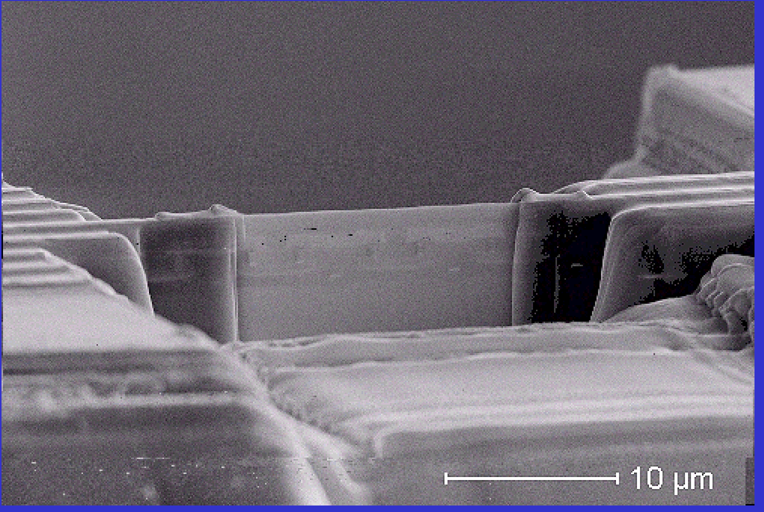

Device Modification

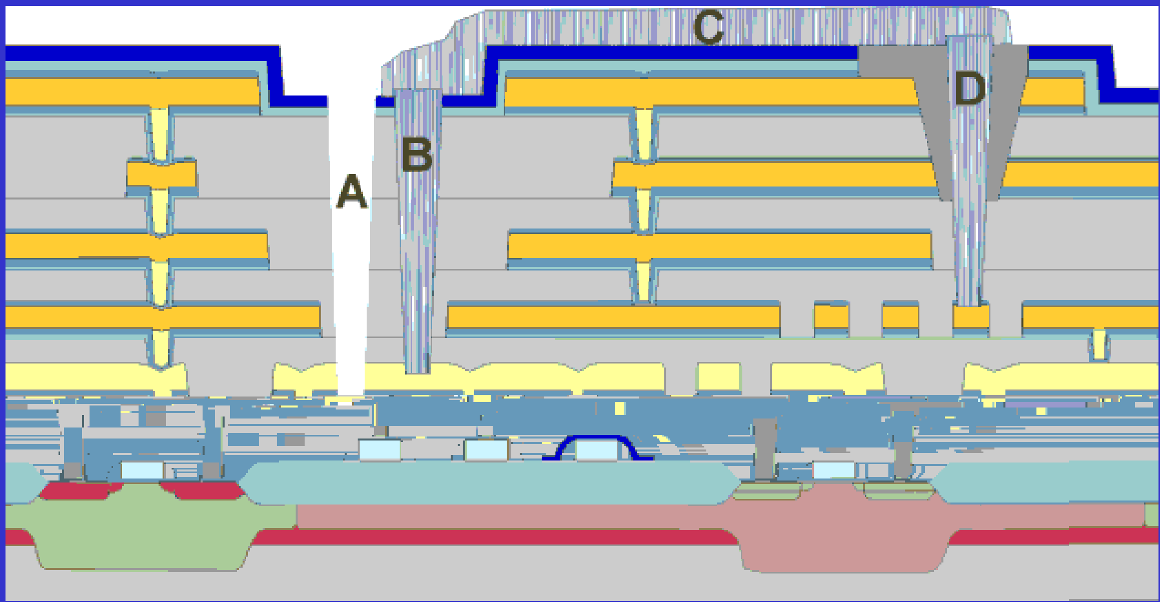

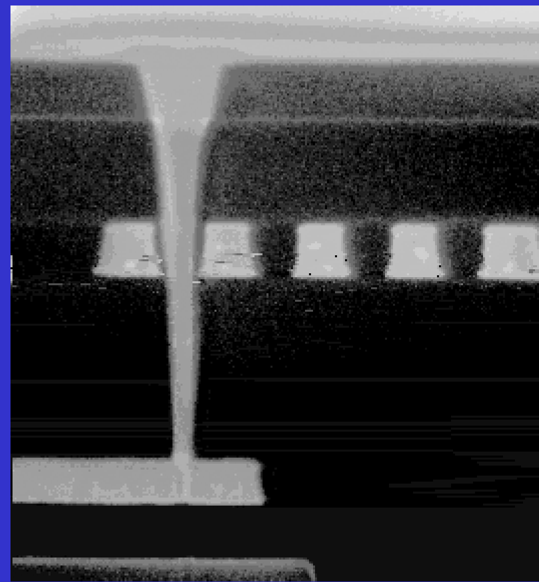

A: FIB cut to metal 1. B: FIB via to metal 1.

C: FIB strap joining vias. D: FIB via to metal 2.

Deep Probe Point Filled with Conductive Material

Other Facilities

Sputtering System

CVD

Reactive Ion Etching

Surface Profile

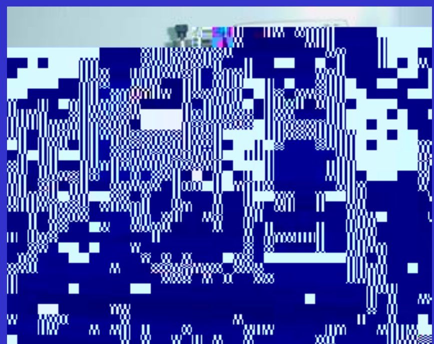

Wire Bounder

Probe Station

SEM

FIB

The processes for fabricating
Pt nanopillar arrays

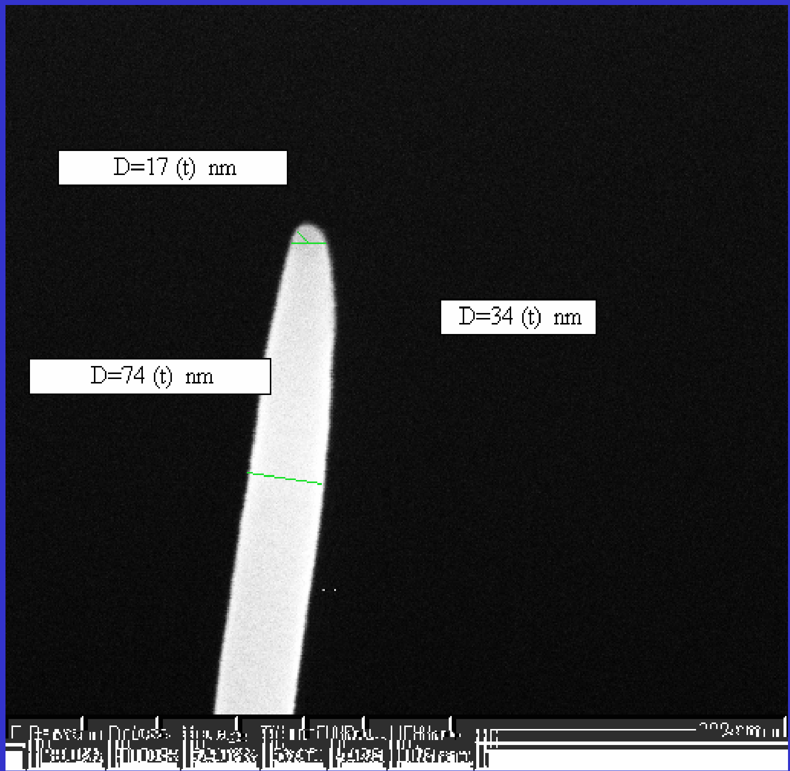

Aspect ratio: 50:1
Tip curve radius:17 nm

After optimization of Pt deposition and milling parameters, the Pt nanopillar arrays with height of 8.5 um and tip radius about 17 nm were obtained.

FE I-V properties of Pt pillars deposited at different accelerating voltages

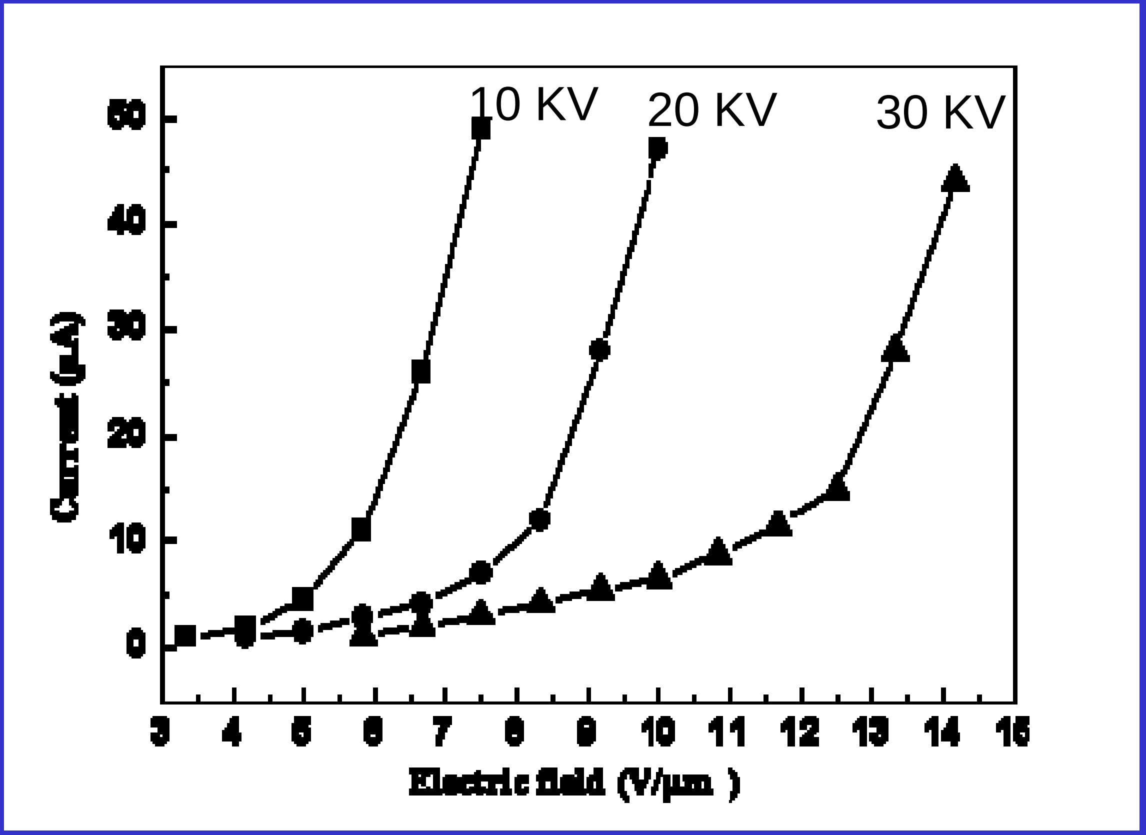

(a) Fabrication process for three-dimensional nanostructure by FIB CVD
(b) Microbeakers with 1,0 and 1.5 um diameter, and 1,0 um height
(c) Microwine glass with 2.75 um external diameter and 12 um height

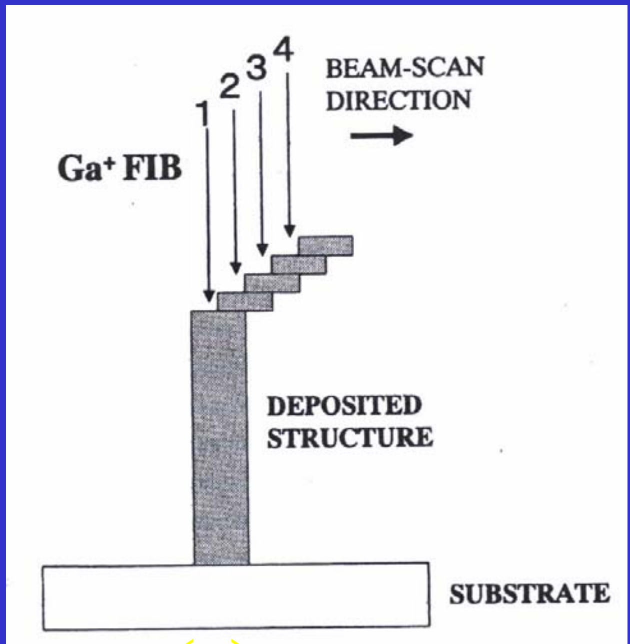

(a)

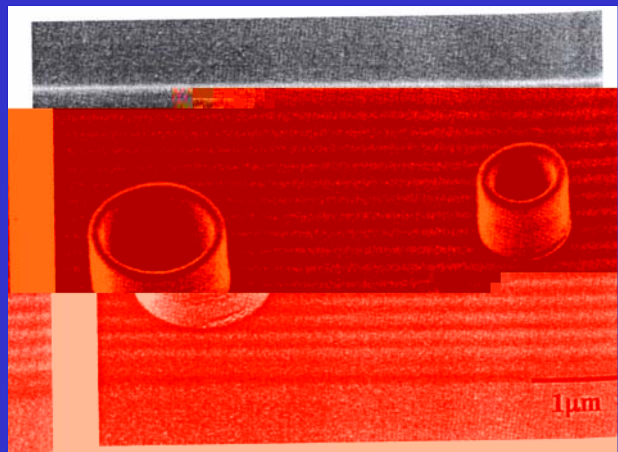

(b)

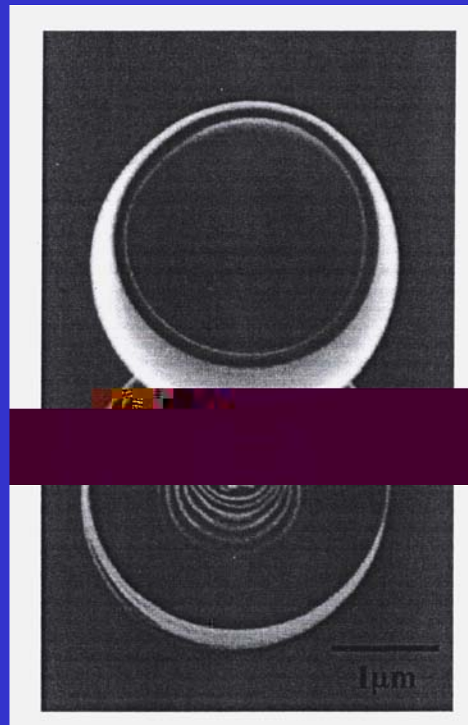

(c)

(a) Microcoil with 0.6um coil diameter, 0.7um coil pitch, and 0.08um linewidth
(b) Microbellows with 0.8um pitch, 0.1um thickness, 2.75 um external diameter, and 6.1um height

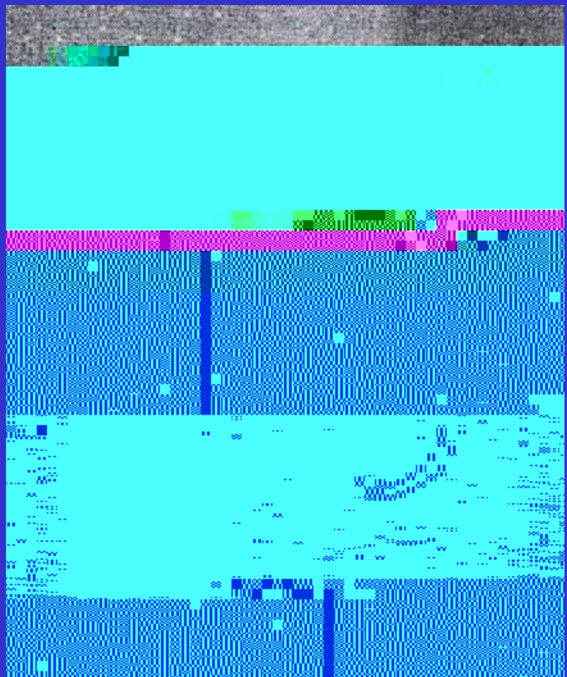

(a)

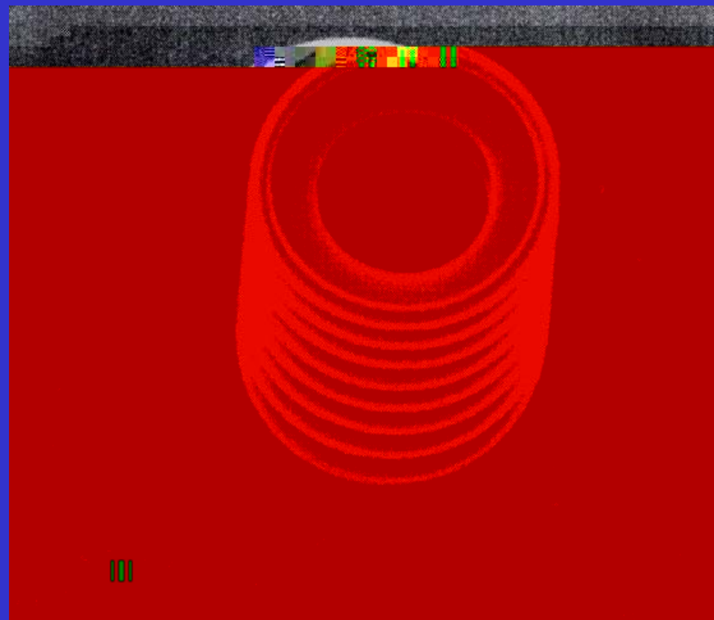

(b)

Quantum lines and dots

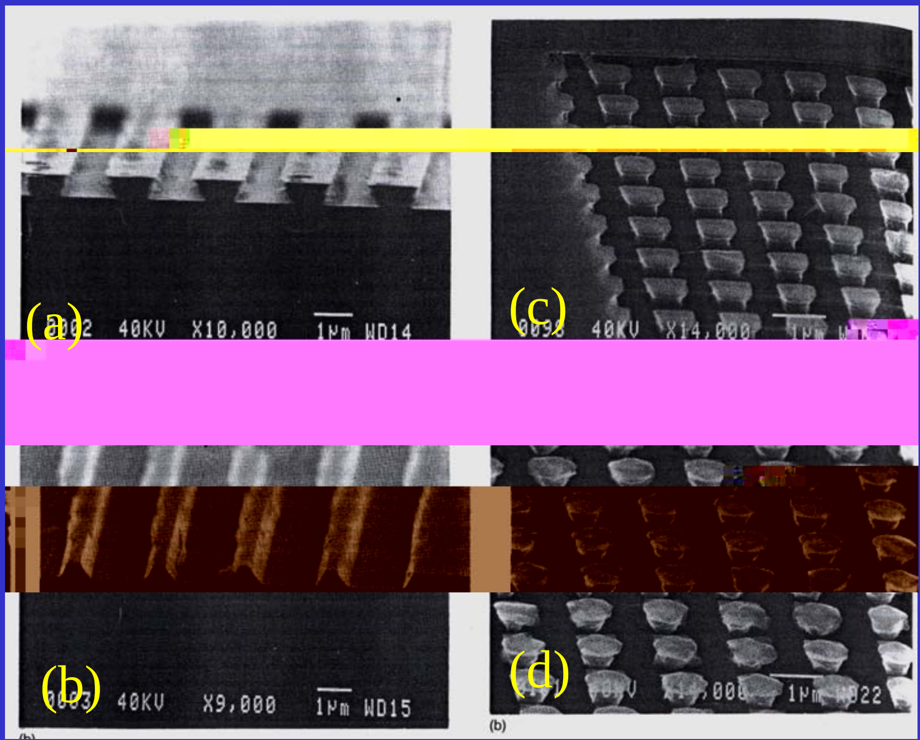

(a) Lines parallel to [110]: patterning width 1 um, period 2.25 um
(b) Lines parallel to [11/0]: patterning width 1 um, period 2.5 um. Note the etch pits on the upper surfacein (a)
(c) dots with exposed regions patterned at 0.5 um, period 1.2 um, etched for 1 min
(d) Dots with exposed regions patterned at 0.5 um, period 1.4 um, etched for 4 min. Note the incomplete etch down to the GaAs stop layerin (c). Some electron-transparaent flakes of GaAs cap layer and QW are visiblein (d)

1.55μm InAs/InP

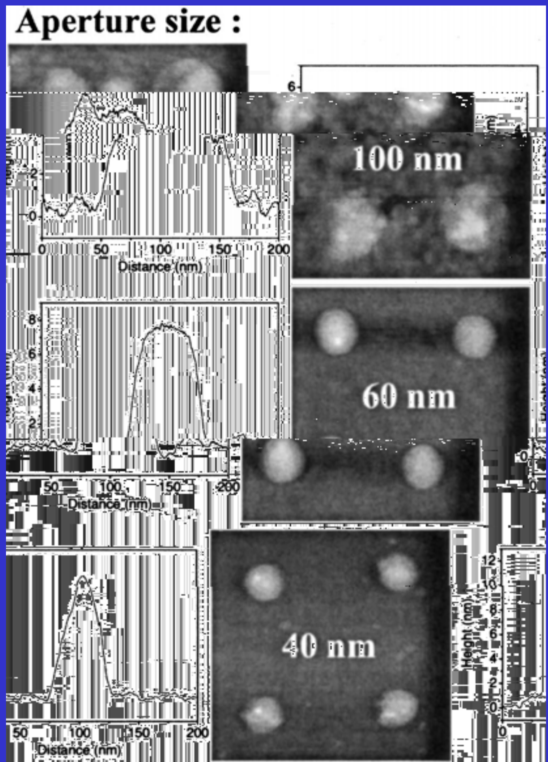

- InAs/InP 1

1 0

- 40-100nm

InAs/InP

- 1.55μm

J. M. Benoit

Appl. Phys. Lett. 88 2006 041113

SEM

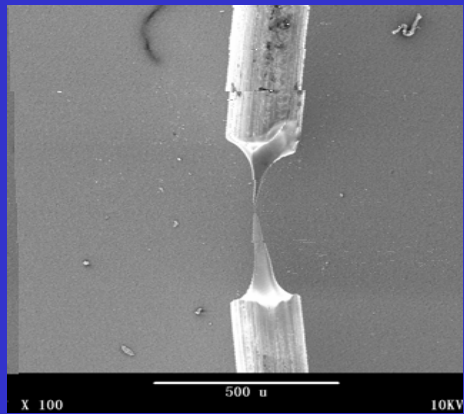

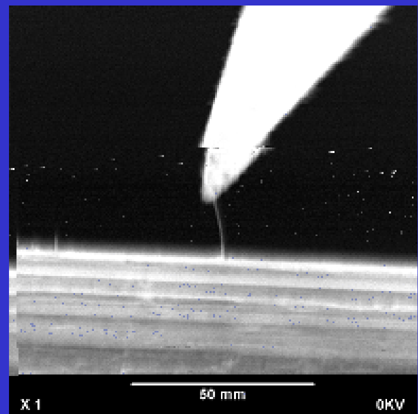

:2003201002228 2002133050.6

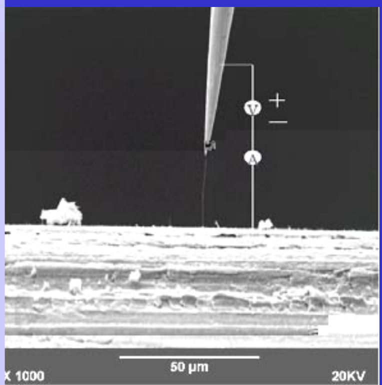

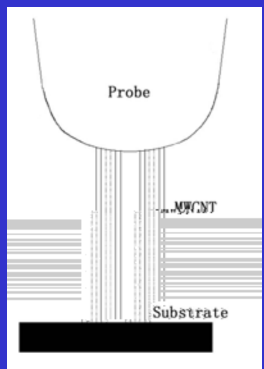

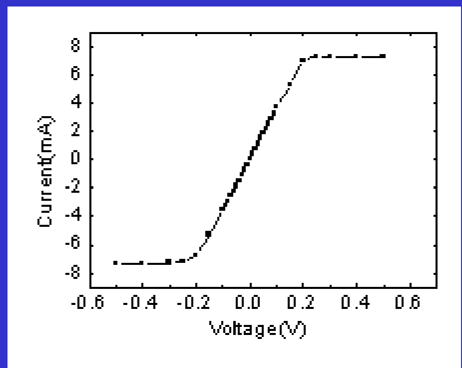

(100nm)

$$f_i = \frac{1}{e^{\frac{E - E_F}{k_B T}} + 1}$$

$$N = \sum_j \sum_i f_{ij} = \sum_j \sum_i \frac{1}{e^{\frac{|E - E_F|}{k_B T}} + 1}$$

7.25mA 460G_0 455G_0

Physical Review Letters 95 2005 086601

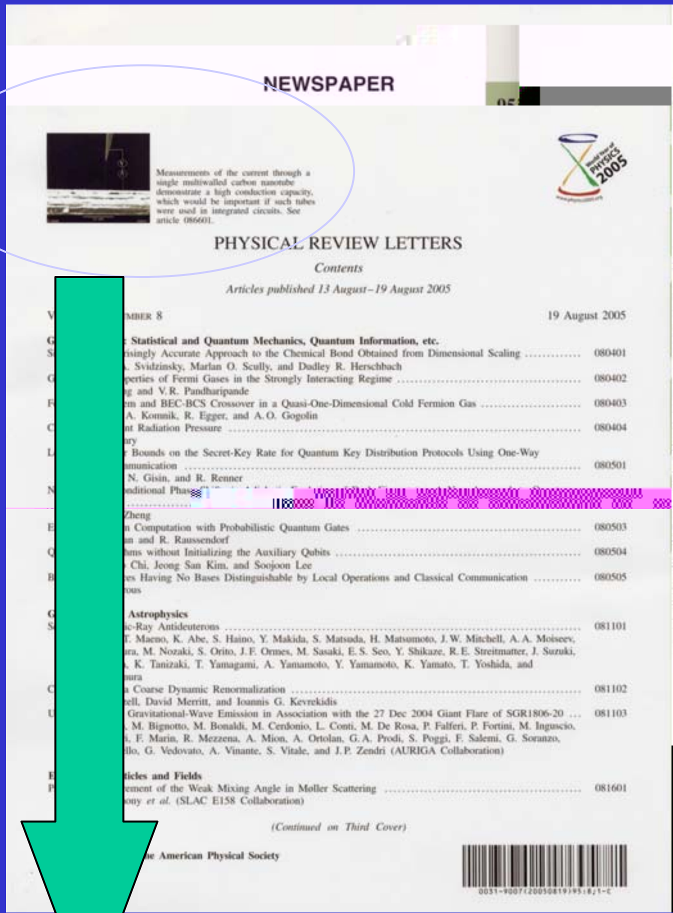

“

”

Three-terminal carbon nanotube junctions: Current-voltage characteristics

L. Liu et al. Phys. Rev. B 71 2005 155424

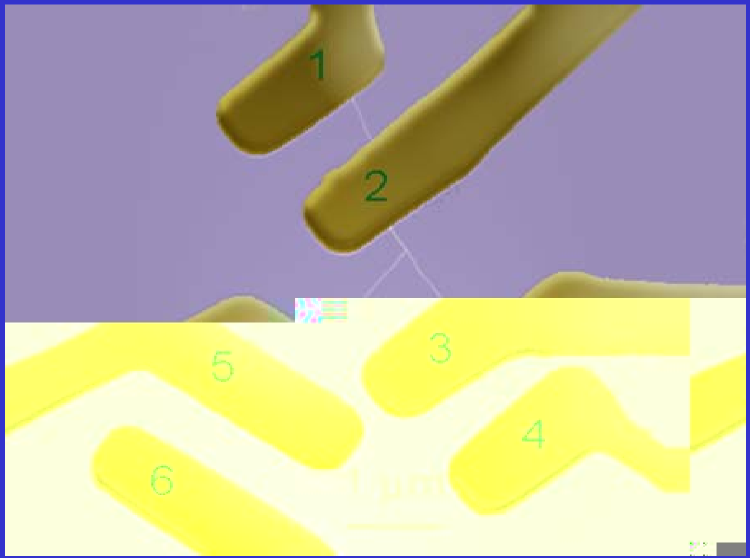

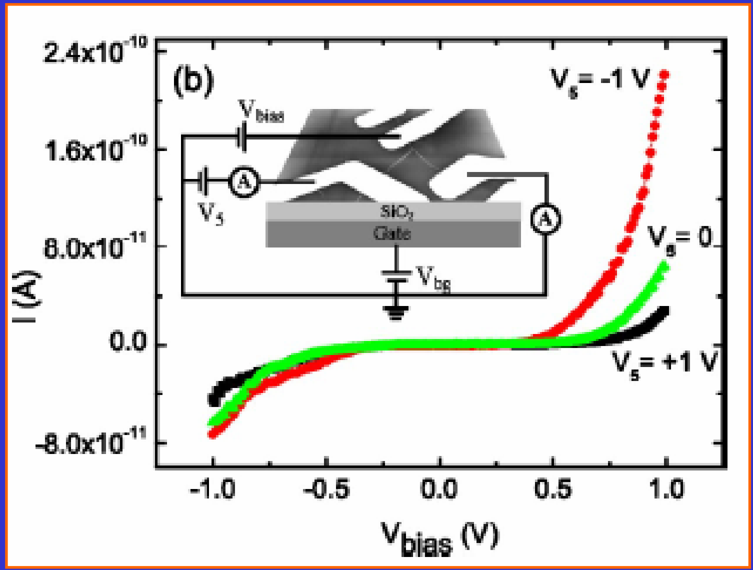

The current in the first nanotube (connected to electrodes 2 and 3) can be influenced by the voltage applied to the second nanotube (connected to electrode 5) which acts as a local gate electrode.

2nm

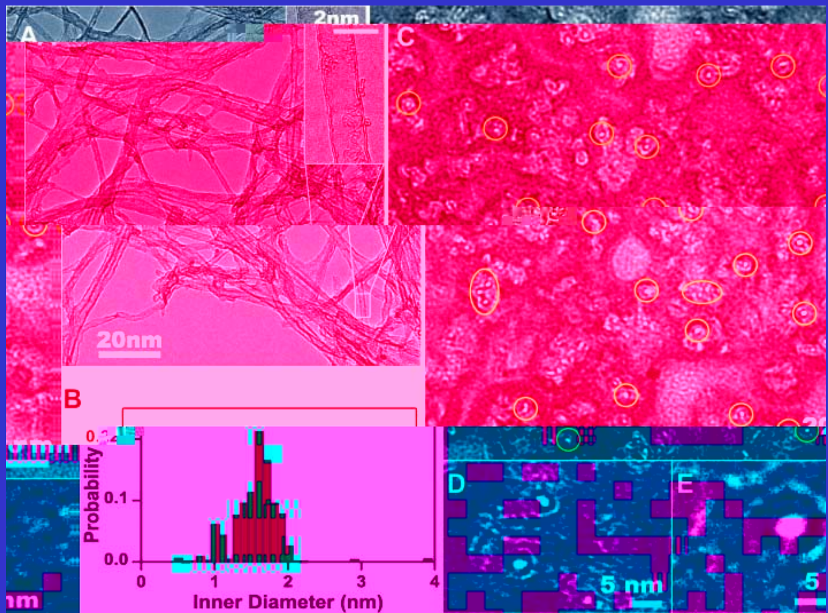

A
2nm
C
20nm
B
Probability
0.1
0.0
0
1
2
3
4
Inner Diameter (nm)
D
E
5 nm

-
-
-

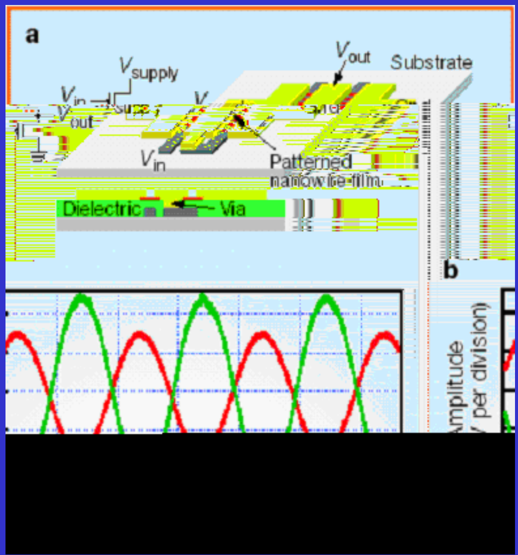

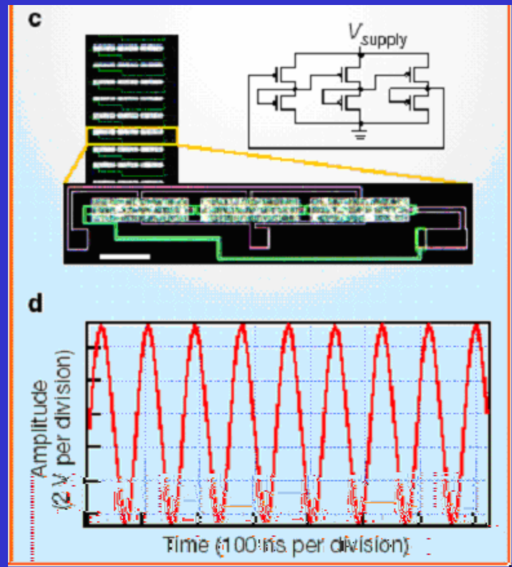

Robin S. Friedman

Nature 434 (2005) 1085

- 10 MHz
  14 ns

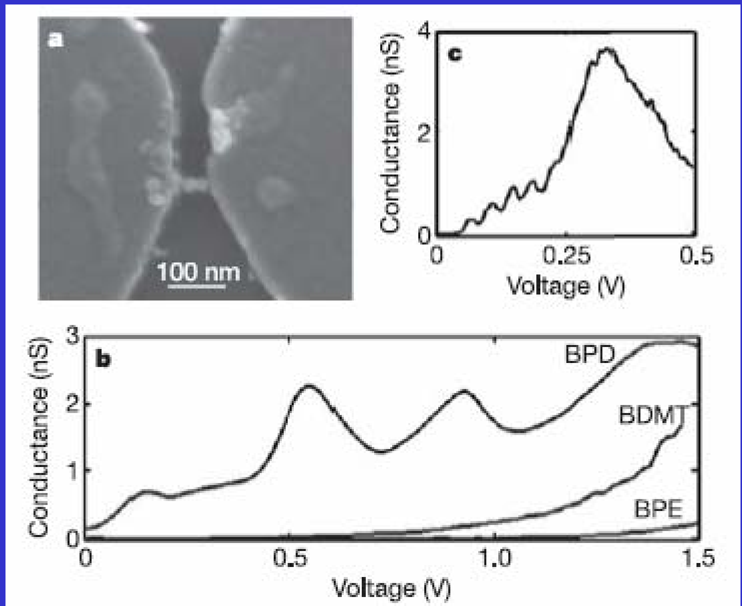

Tali Dadosh

NATURE677 2005 **436**

- SH
-
- BDP BPE, BDMT

EBL

- BPD BPE BDMT

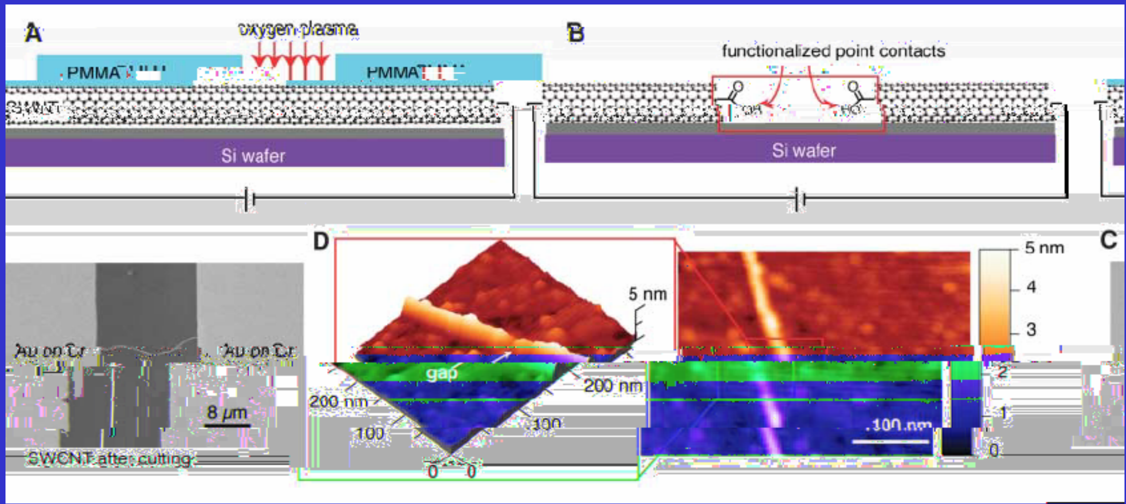

Xuefeng Guo

Science
311 (2006) 356

•

•

10 nm

•

pH

Yuanbo Zhang

Nature 438 (2005) 201

•

,

Berry

•

•

Berry

- MTJ
-
-

The test structure of ferroelectric properties

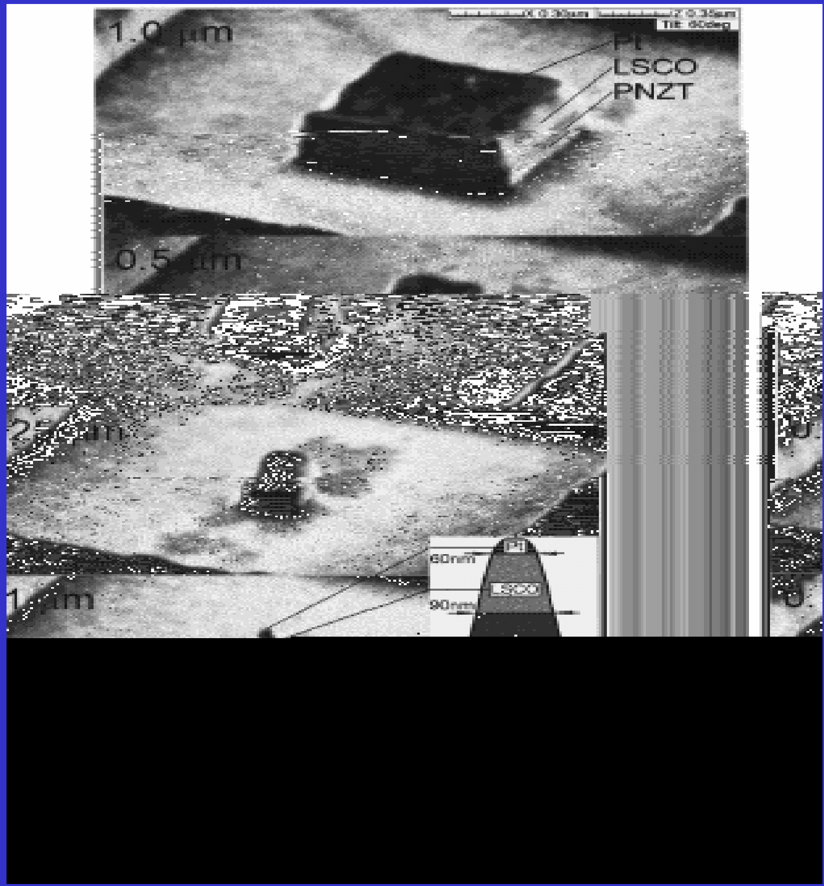

FIB milling in the size range from 1um^2 to 400 nm^2

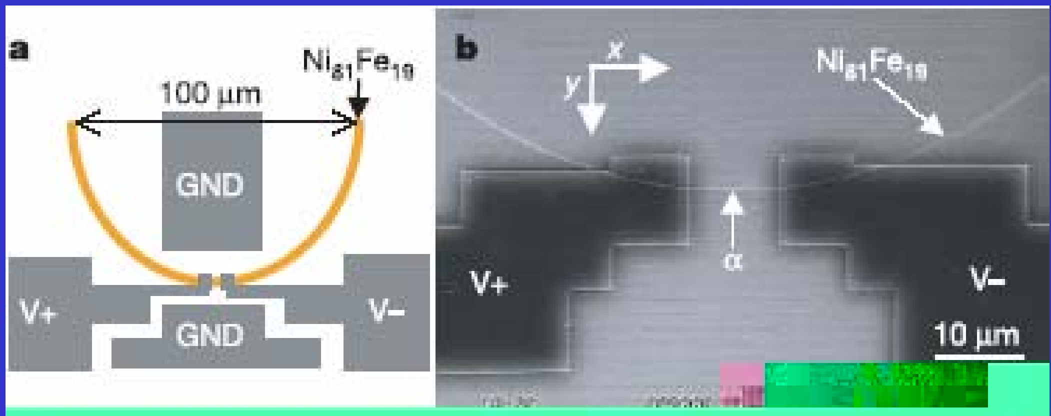

J. Saitoh

Nature 432 (2004)203

-
- Ni81Fe19
-
- 6.6 × 10-23 kg

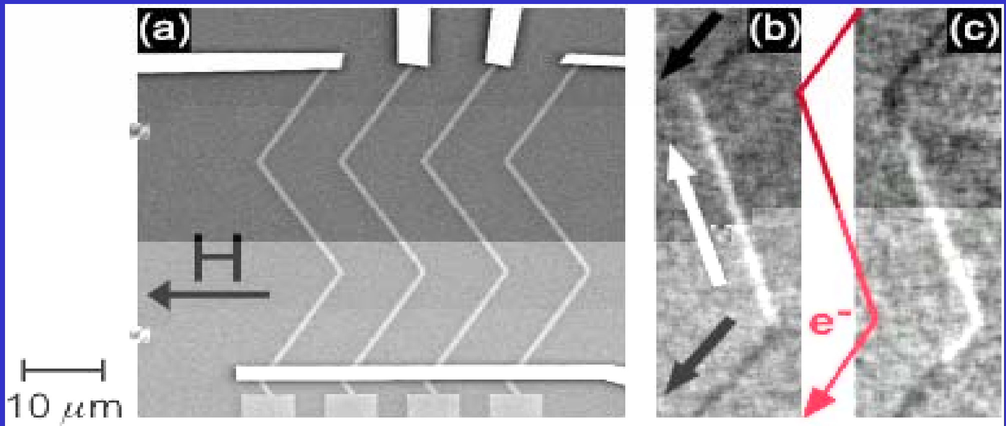

Kläui
Physical Review Letters
95 2005 026601

•

• Ni80Fe20
100nm 500nm

• 500nm 10nm Ni80Fe20
0.3m/s

Submicrometer Ferromagnetic NOT Gate and Shift Register

D. Allwood, Science, 296(2002)2003

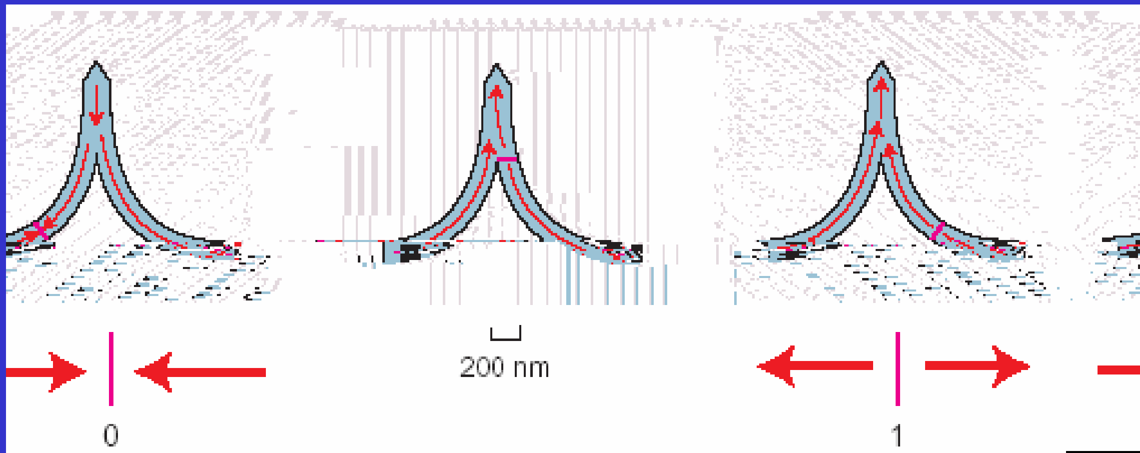

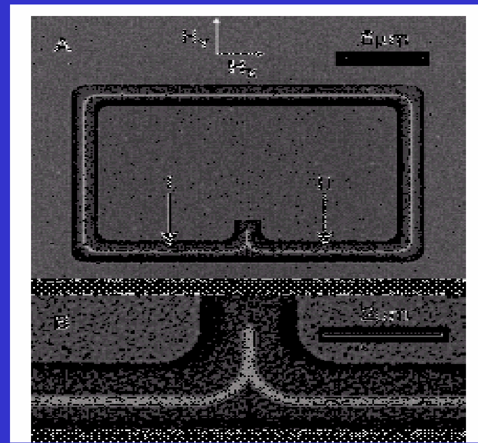

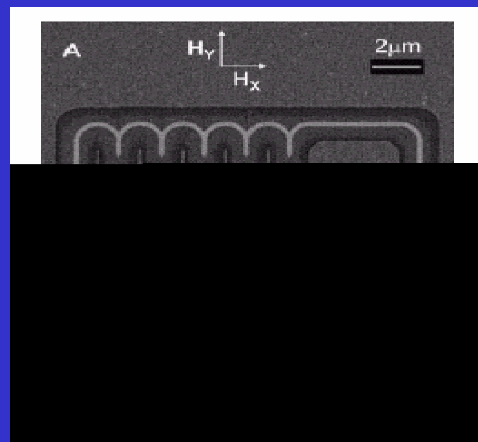

A rotating magnetic field changes the value of a bit by moving and then flipping the boundary between regions of magnetized wire.

-
- metamaterials)
- Plasmon
-

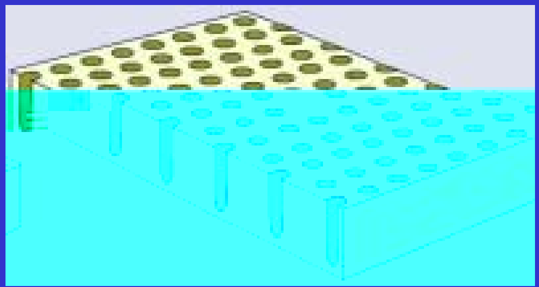

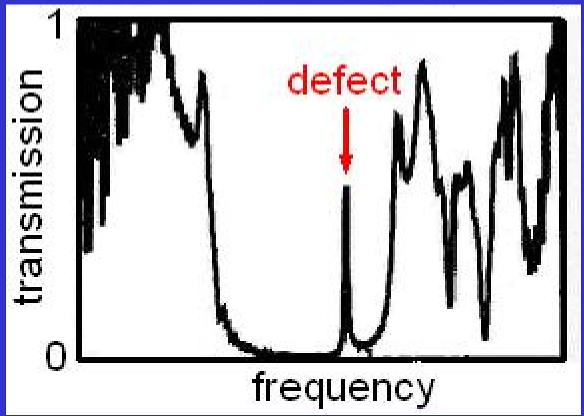
1
0
transmission
frequency
defect

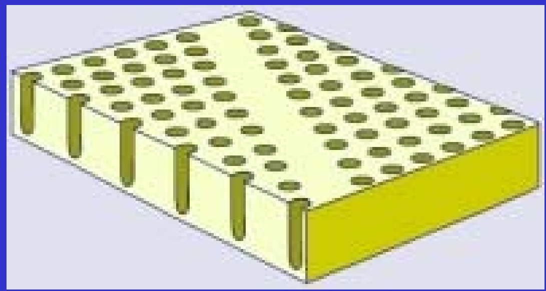

Butterfly Scales as Living Photonic Crystals

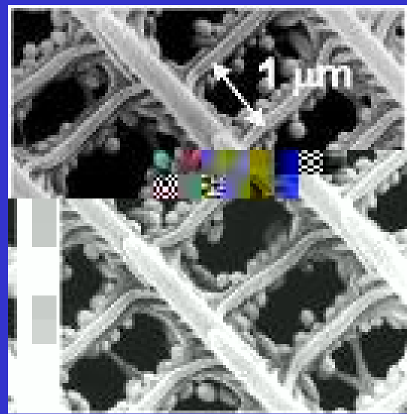

port1 port2

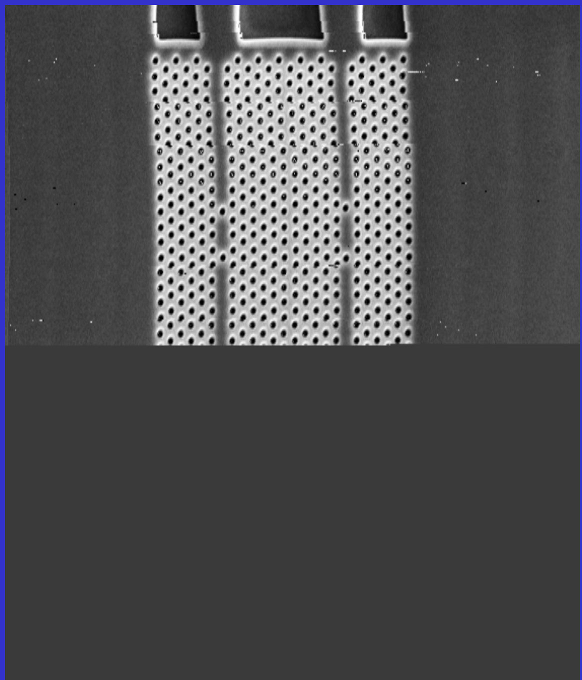

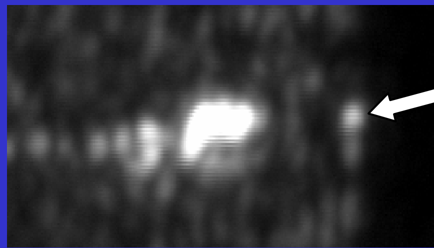

1572nm

1567nm

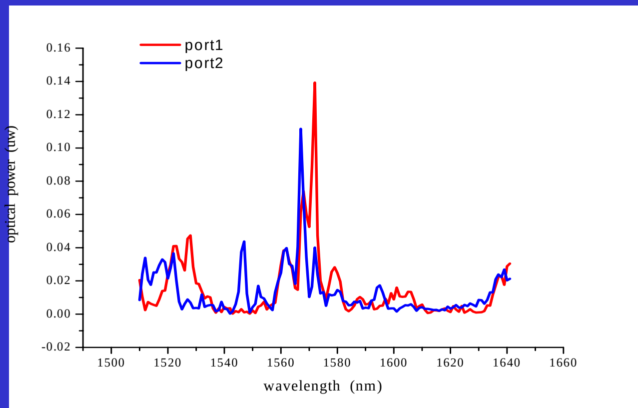

，

5nm

Left-hand materials (LHM)

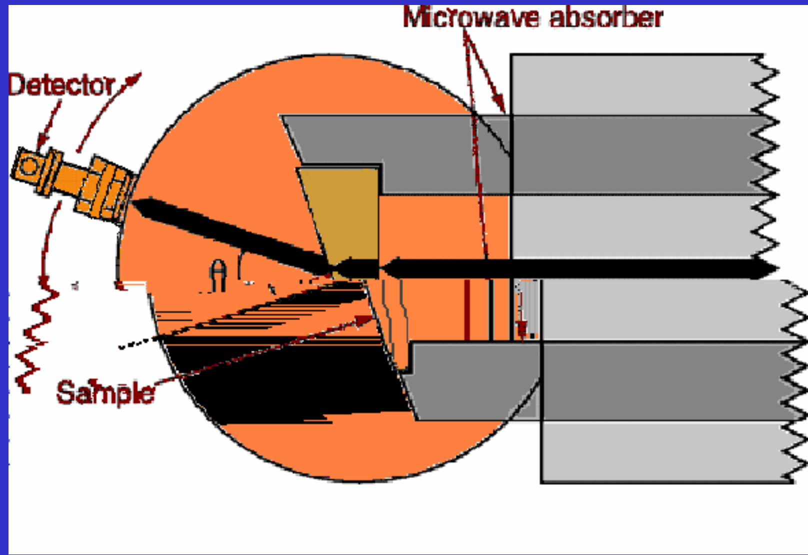

D. R. Smith
Science **292**(2001) 77

Snell
Doppler
Cerenkov

100 THz

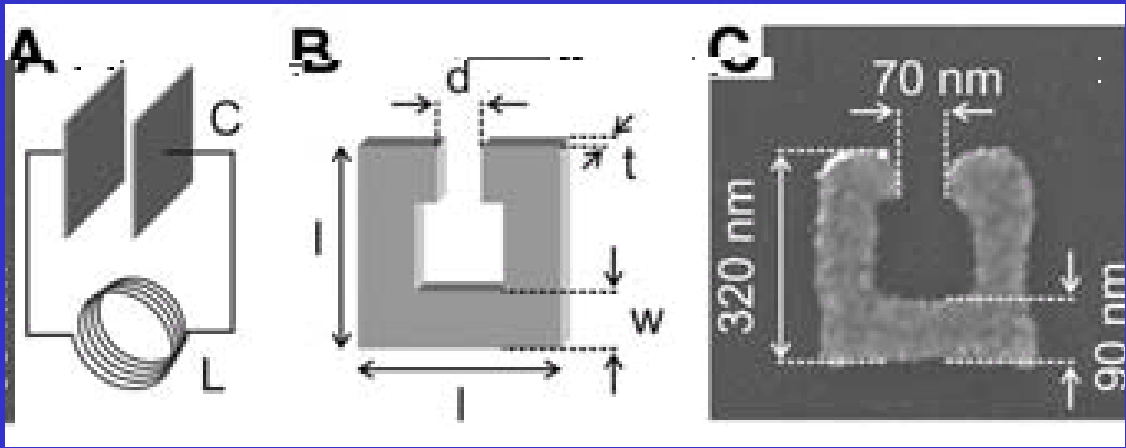

Stefan Linden

Science
306 (2004)1351

•

• LC

1 THz

THz

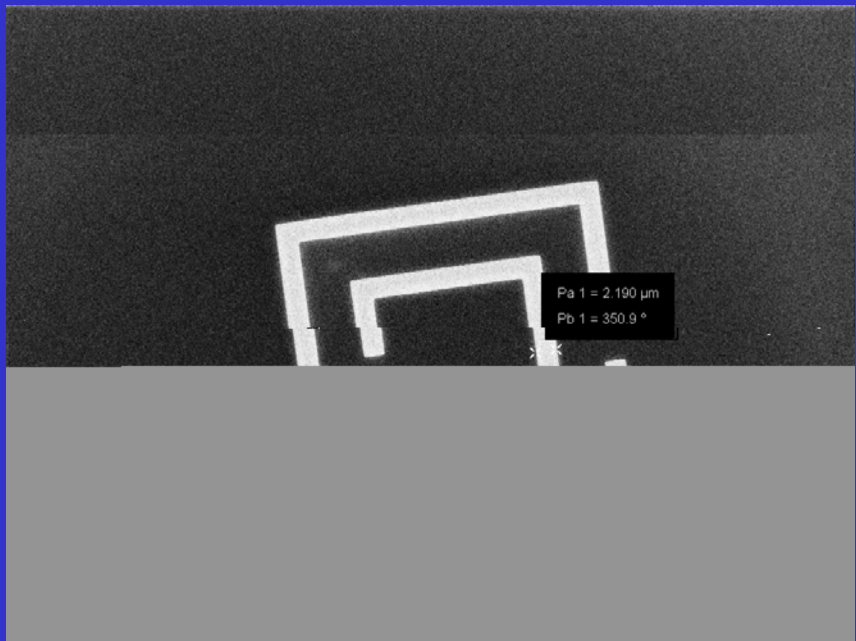

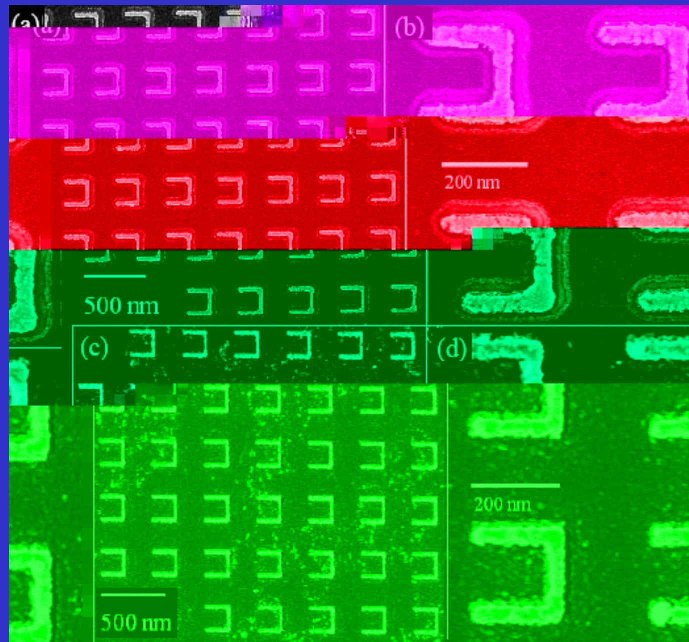

THz

:

.

Beaming Light from a Subwavelength Aperture

60nm
100%
650nm

SCIENCE
2002 VOL 297

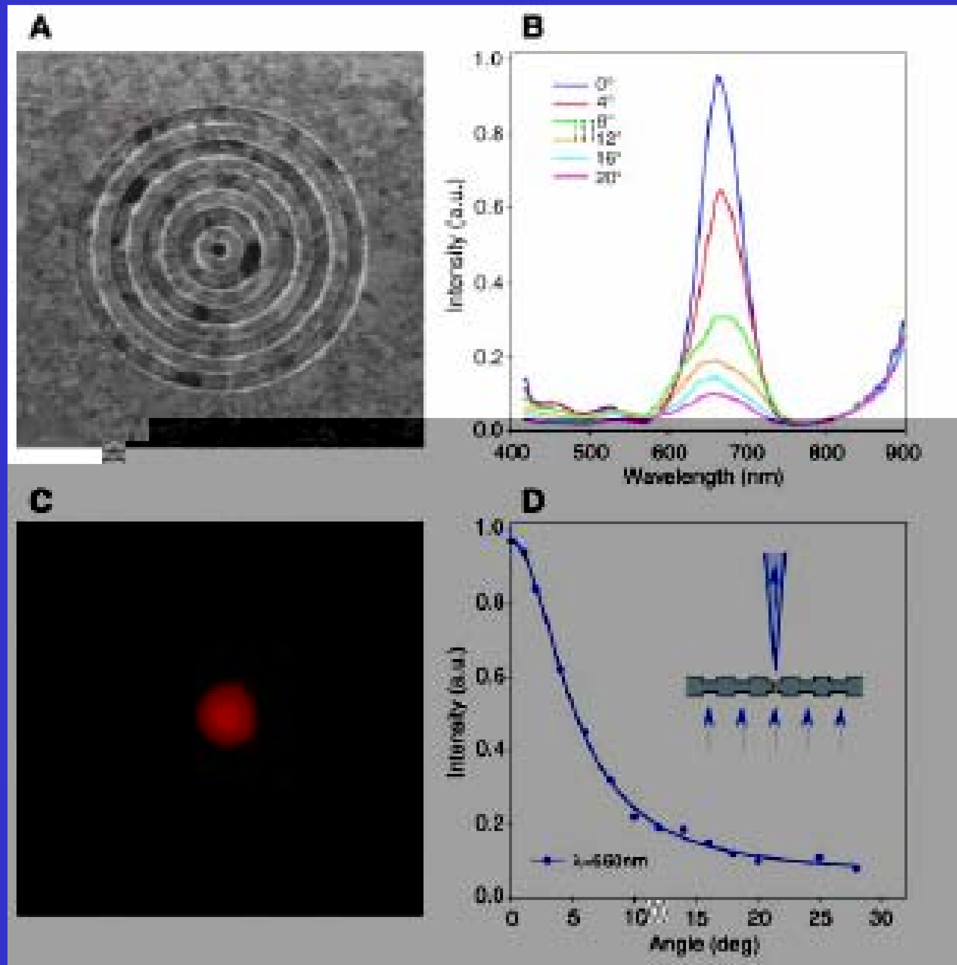

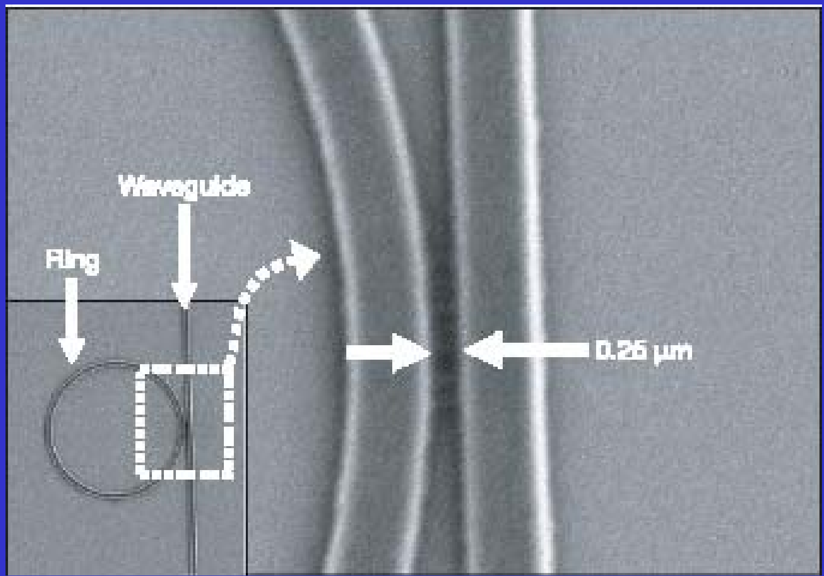

V. R. Almeida

Nature 431 (2005)1081

•

• SOI

•

25 pJ

500 ps 94%

ε

控制电磁波实现隐身

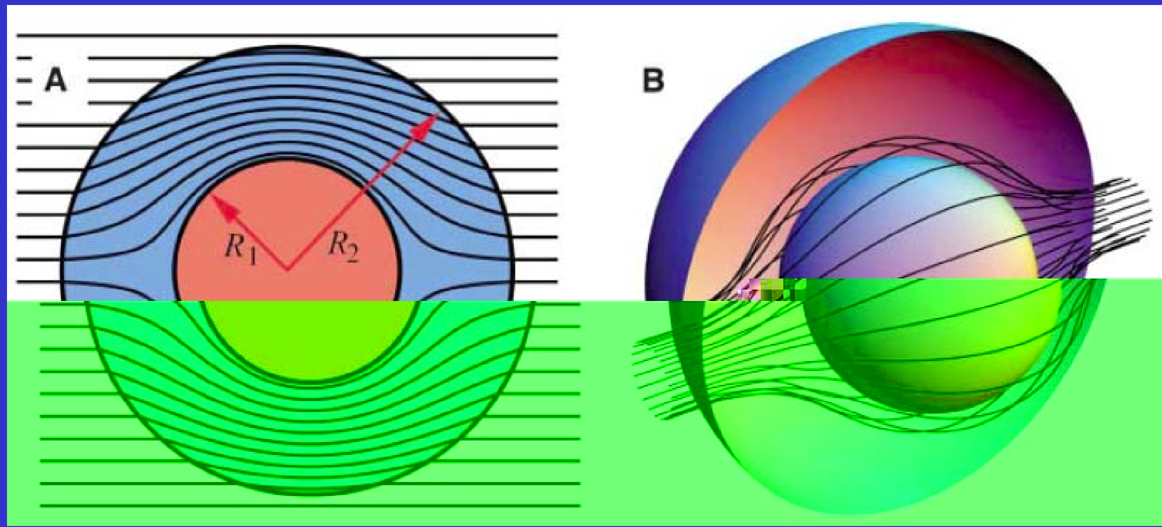

Science, 312 (2006)1780

ε

微波隐身材料

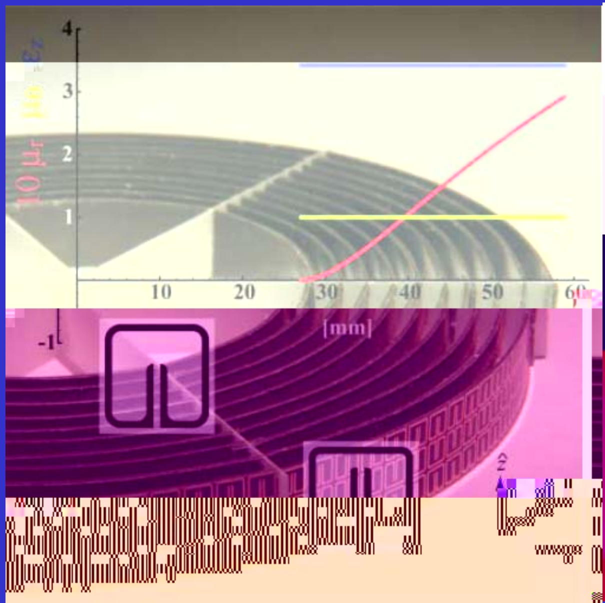

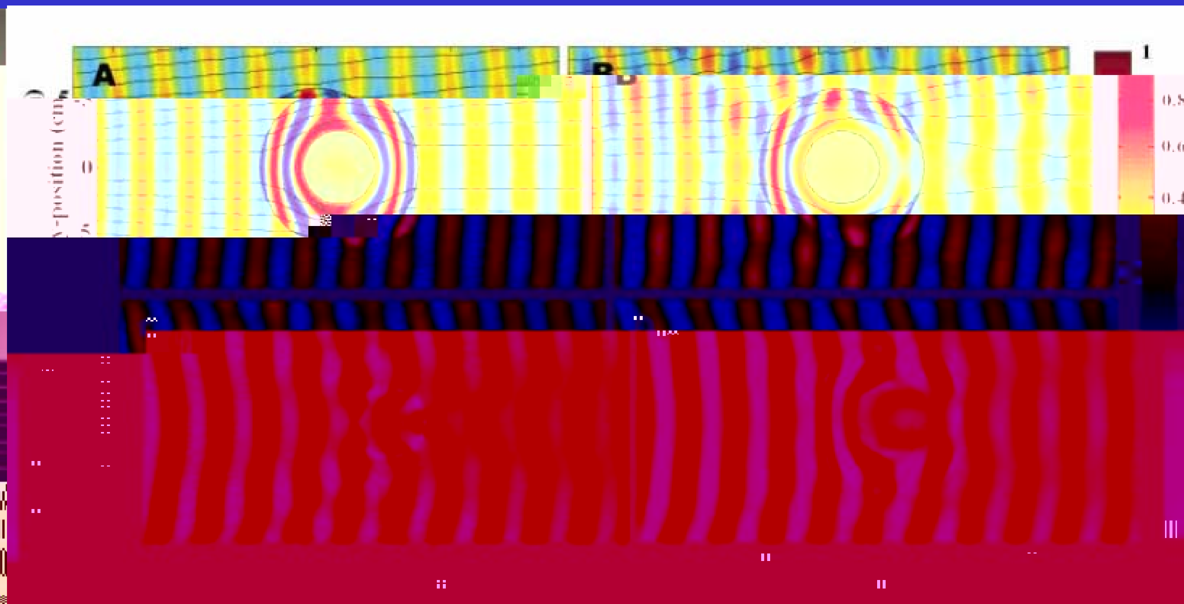

Science (2006)

ε

红外与可见波段的隐身

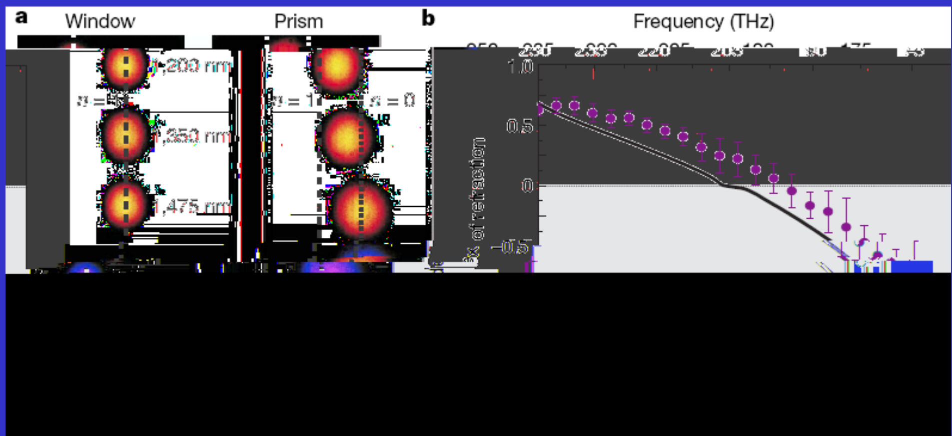

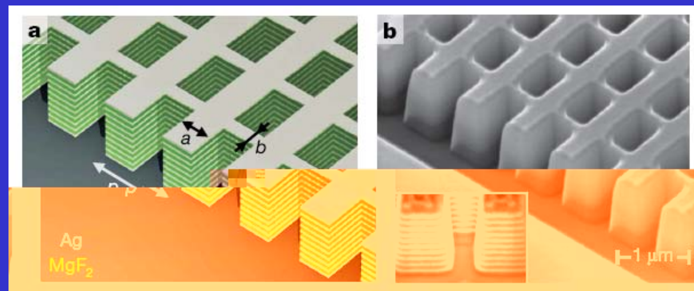

MgF_2/Ag

1475nm 0

Nature (2008)

DNA detectors

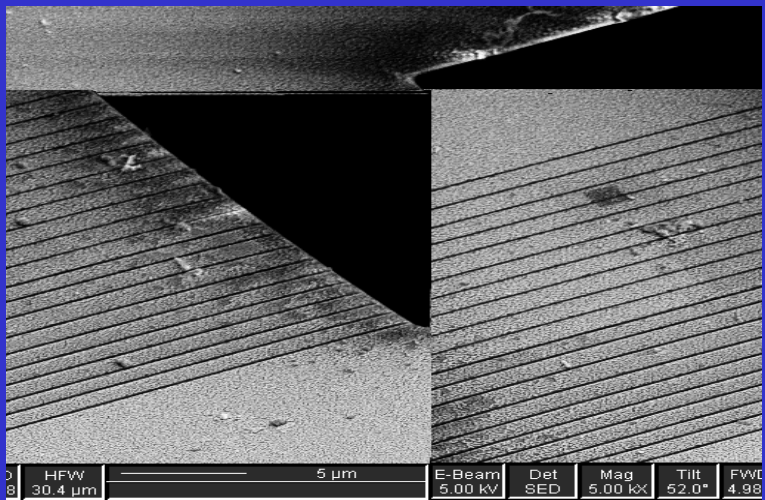

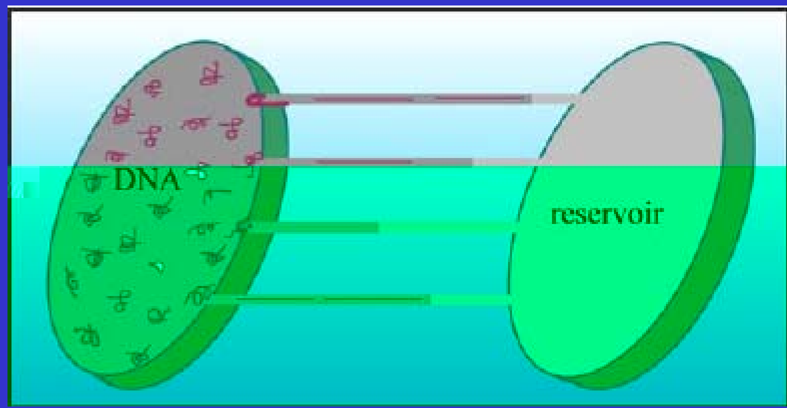

DNA

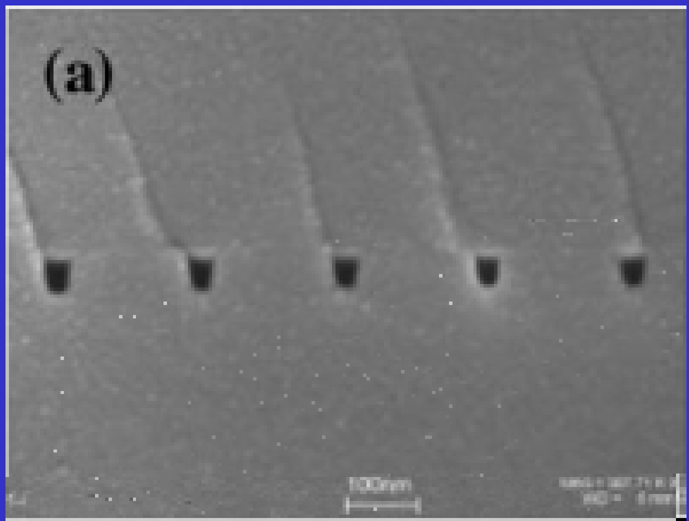

Walter Reisner

Physics Review Letters
94 (2005) 196101

- DNA
- 30-400nm
  -
  DNA
- “ ”
  DNA
  de Gennes

An all-metallic magnetic logic gate fabricated by Invar nanostructures

Introduction

Spin injection

- external magnetic field
- spin-polarized current

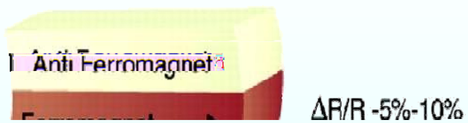

The nanoconstriction structures

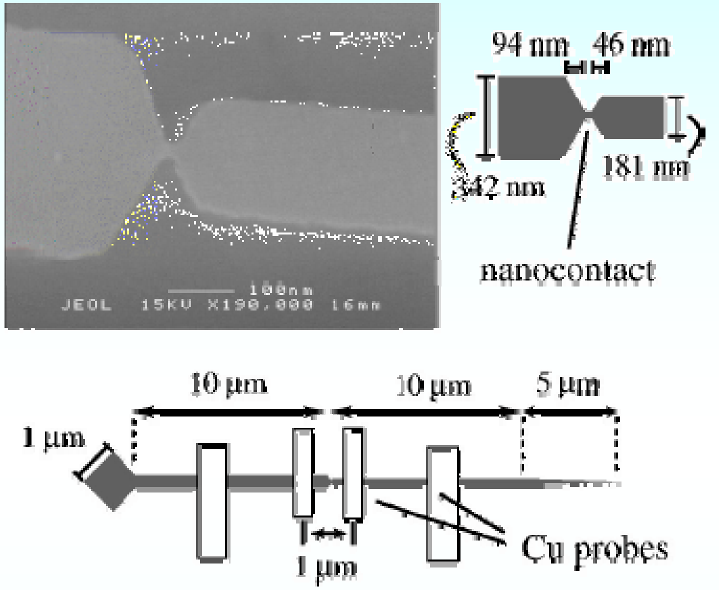

FIG. 1. Schematic illustration of the shape of a typical sample and the SEM image of the nanocontact between two wires. The narrowest square between two wires is defined as "nanocontact" in this article. The size of the nanocontact estimated from the SEM image was 13×13 nm^2.

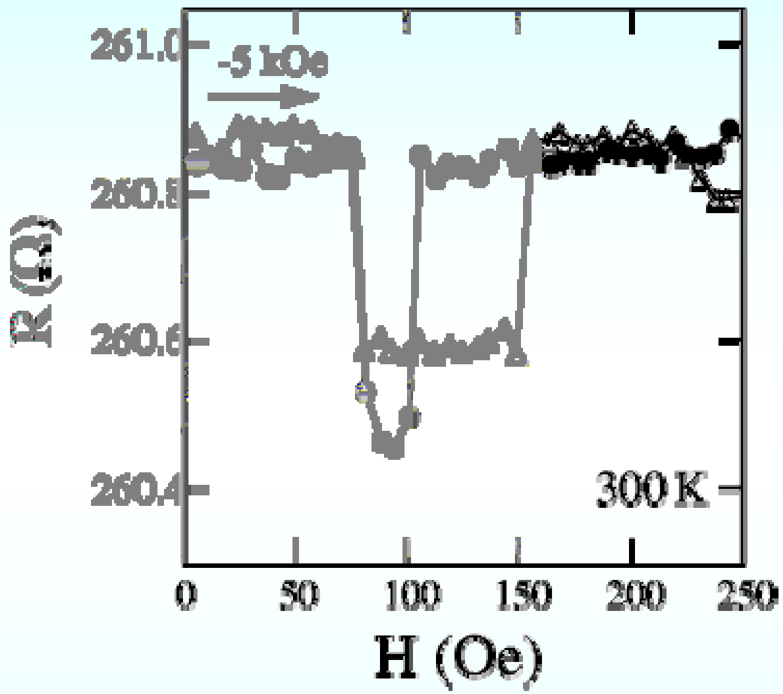

MR measurements. Micromagnetics simulation showed that a trapped DW at the nanocontact has an internal magnetic structure similar to a Néel wall inside the nanocontact. Two

K. Miyake et. JAP 97,014309(2003)

Domain wall motion in metal and semiconductor

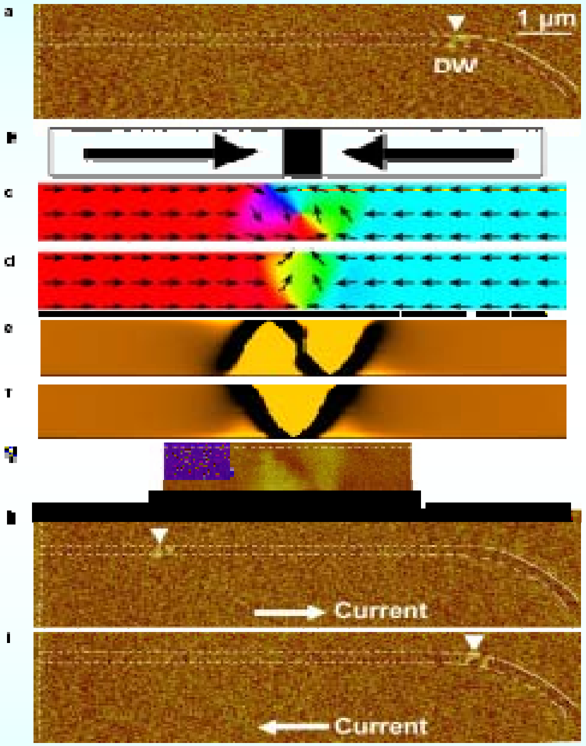

Yamagushi et al., Phys. Rev. Lett. (2004)

Yamanouchi et al. Nature 428(2004)539

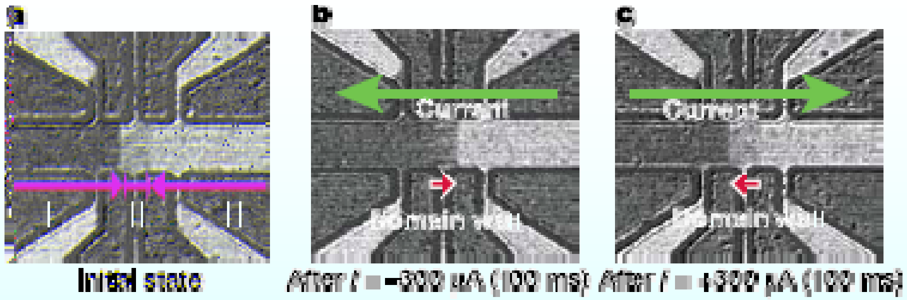

Observation Domain wall motion in nanostructure

Invar alloy nanocontacts

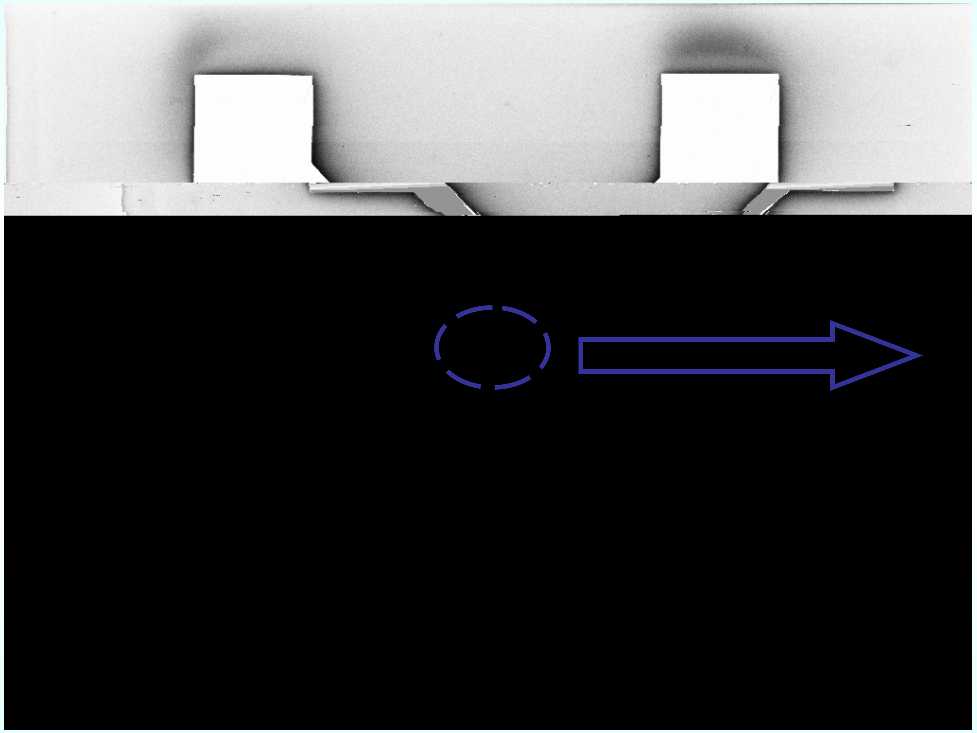

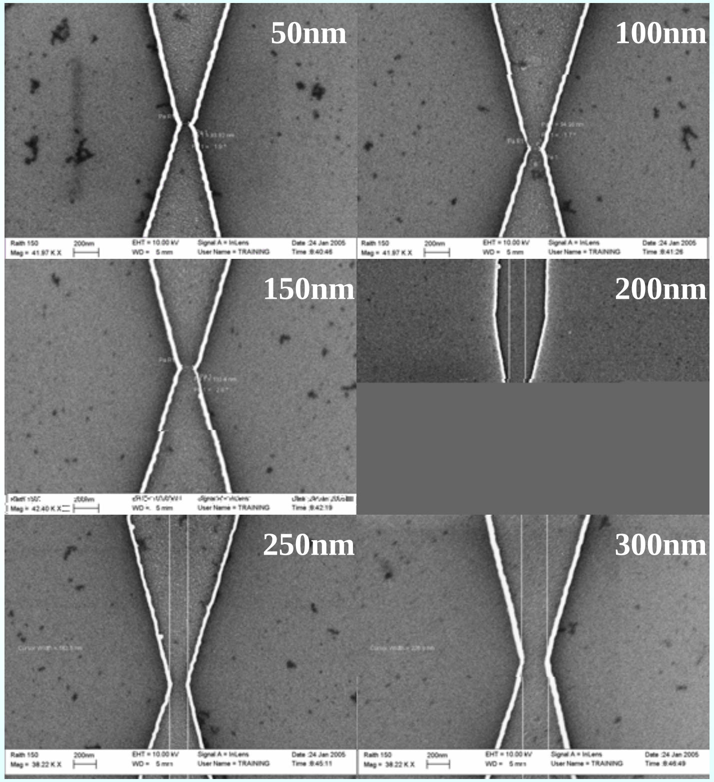

Different widths of Invar alloy nanocontacts and the measurement electrodes

Gu et al. APL 88 2006 033108

Domain wall magnetoresistance

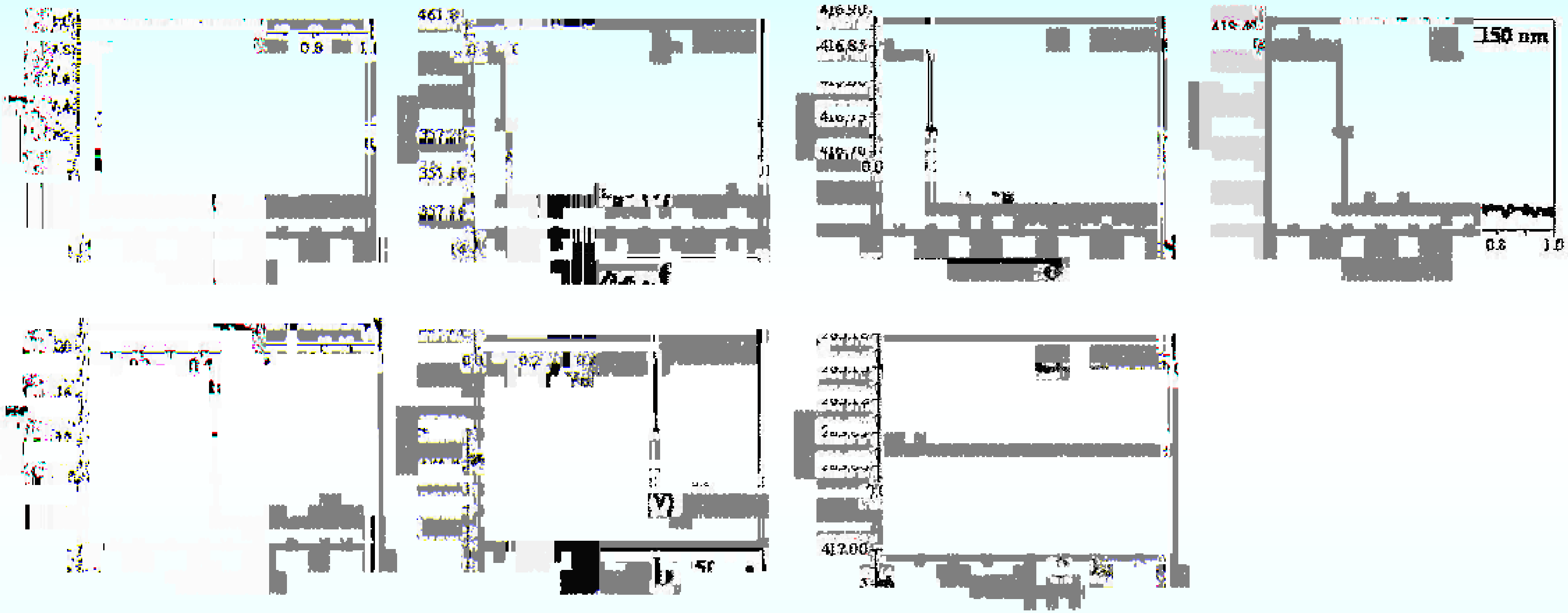

- nanocontact can pin a domain wall
- the change of resistance is DWMR
- DWMR decrease with the increasing width
- critical current increase with the increasing width

Domain wall magnetoresistance

"domain wall displacement by spin polarized current"

L. Berger J. Appl. Phys. 55,1954(1984)

"spin pressure"

J.M.D. Coey Phys. Rev. Lett. 87,026601(2001)

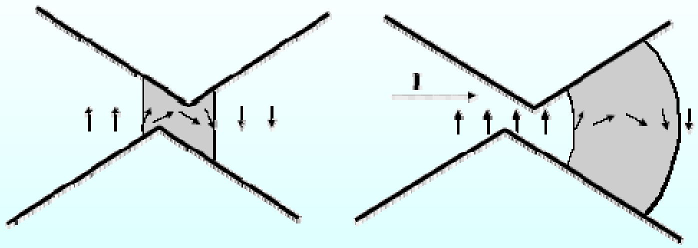

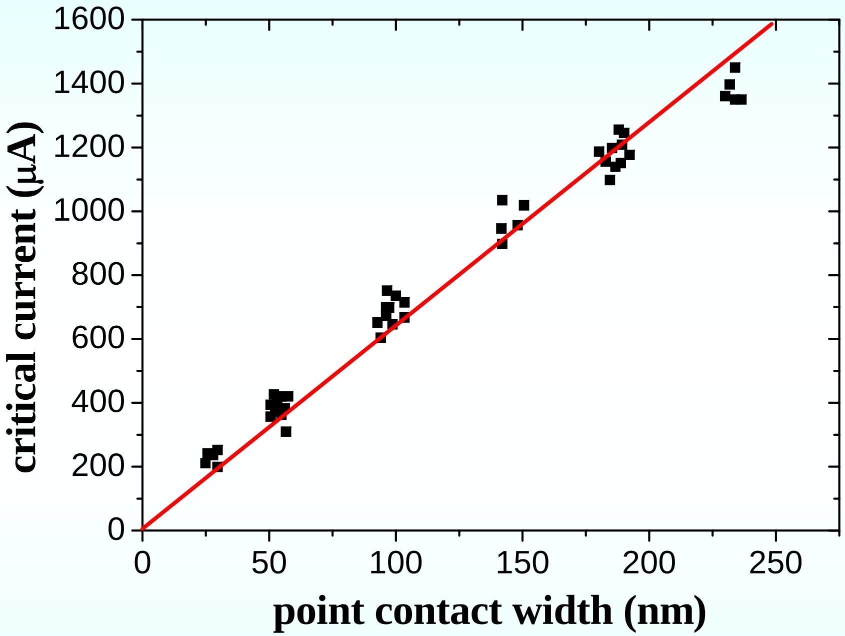

The current density required to be of the order 1.8E7 A/cm^2

(agreement with the observations in bulk materials)

Micro-Magnet Simulation (OOMMF)

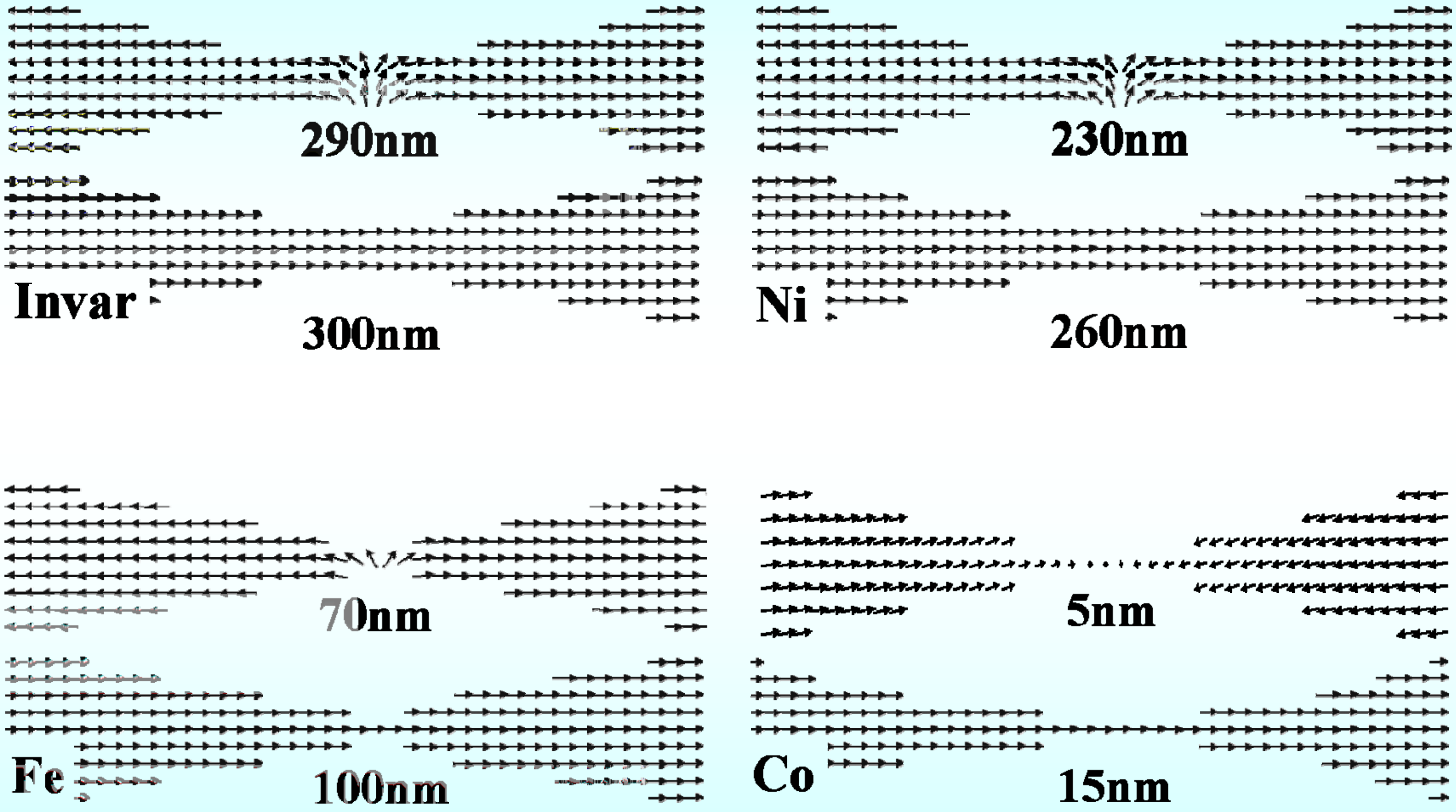

Agreement with above experimental results

Critical current and coercive force

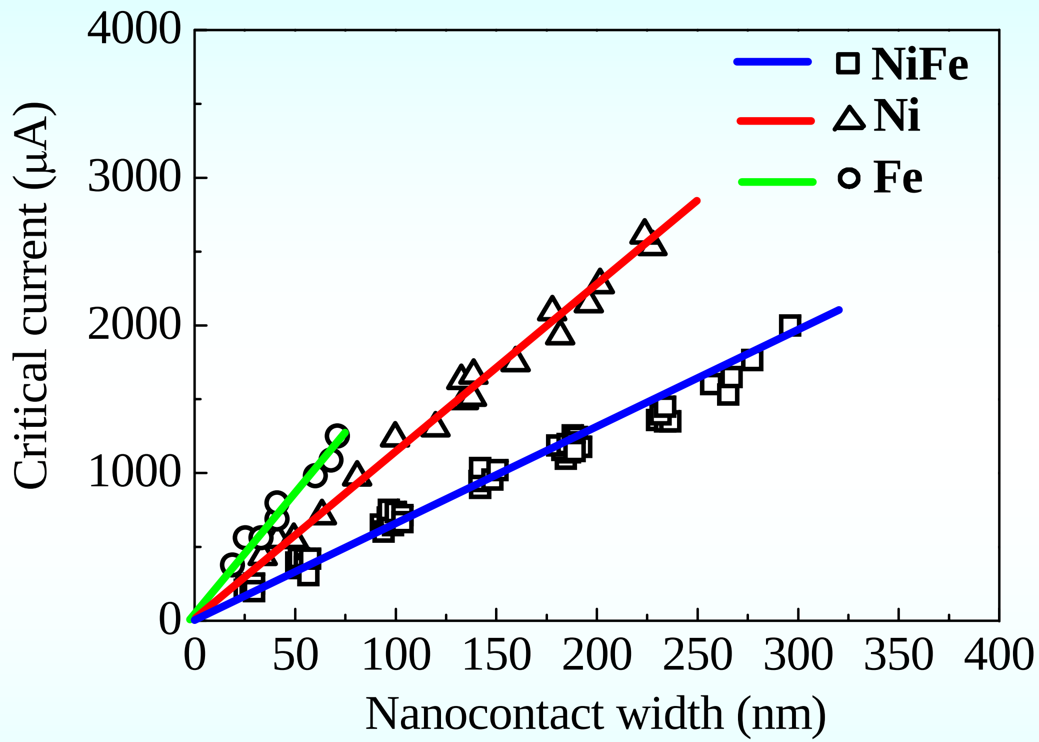

"spin pressure" by spin polarized electron:

$P \propto J\ \tau_{sr}\Delta/e\delta$

Critical depin pressure:

$P=\pi^3 Am/2S$

$J \propto \pi^3 Ame\delta/2S\tau_{sr}\Delta$

NiFe	Ni	Fe	Co
0.05 Oster	0.7 Oster	1 Oster	10 Oster

Critical current increases with the coercive force

The direction of DW motion

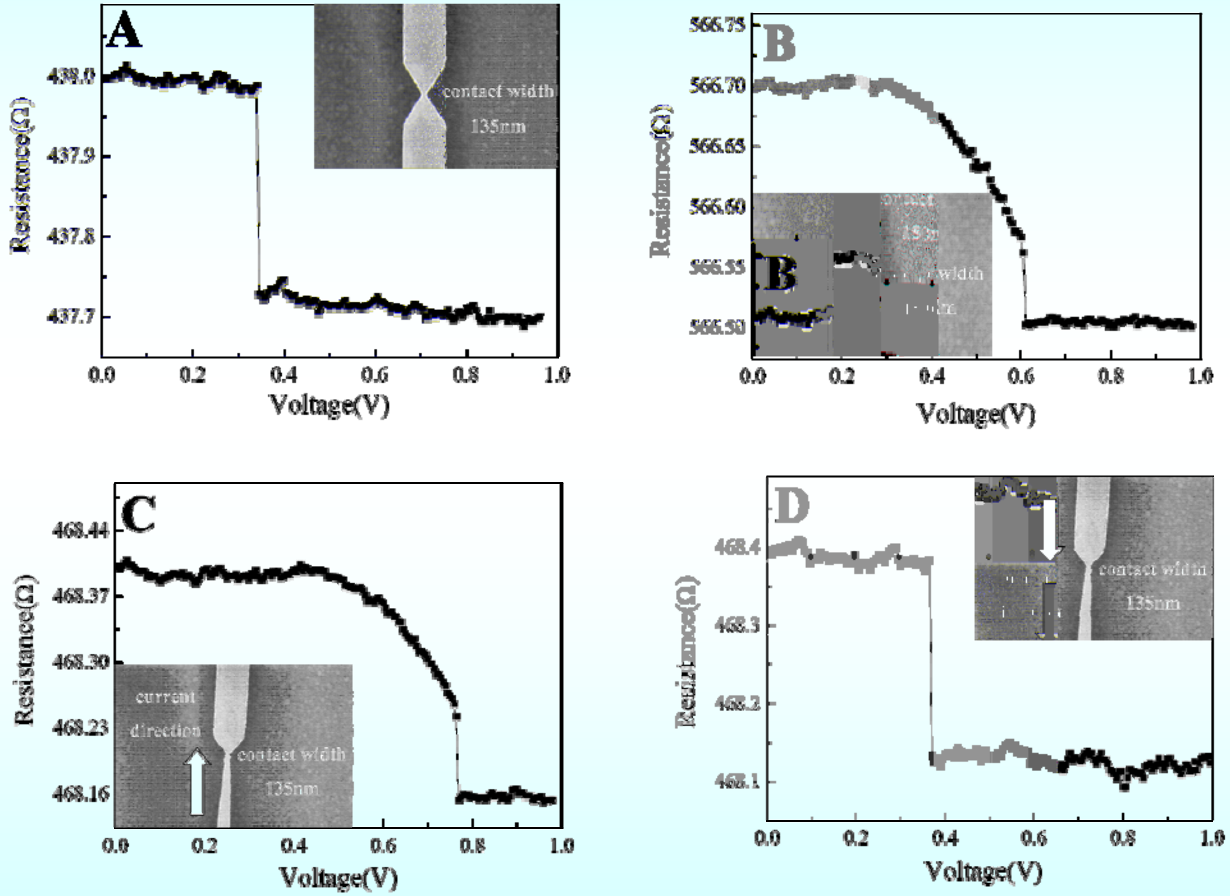

Resistance change in different structures

Direction of DW motion is the same to that of current carrier

Gu et al Nature Nanotechnology 3 2008 97

Alternating Current resistance spectra

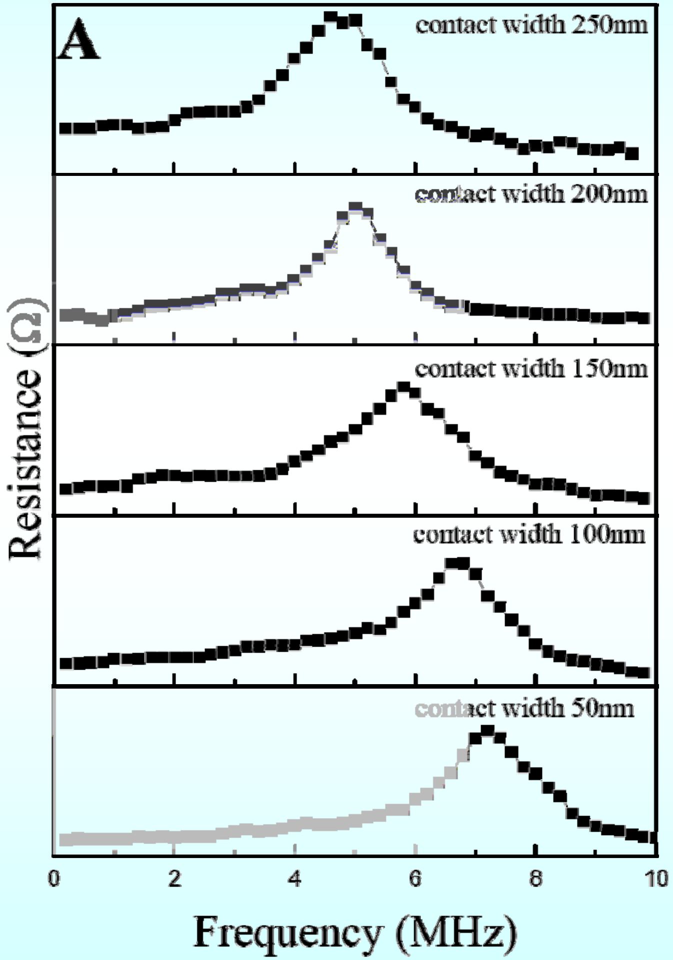

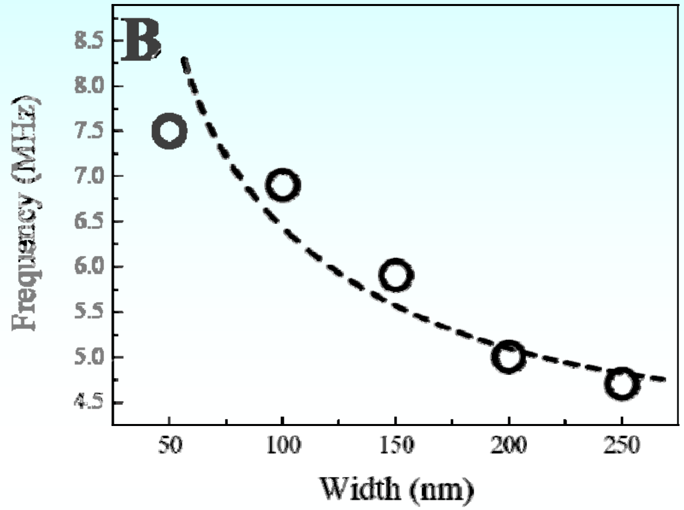

small oscillation

$f^2=k/m$

$m=h^2N/(4\pi^2KW^2)$

$f\sim 1/W^{1/2}$

Contact width is a important parameter for controlling the resonance frequency

Gu et al. Nature Nanotechnology 3 2008 97

Fitting results

$$\Delta\,\mathrm{R}(f) \qquad \frac{1}{8\pi^2 m\tau I^2}\frac{f^2\left|F(f)\right|^2}{\left(f^2 - f_e^{\,2}\right) + \left(f/(2\pi\tau)\right)^2}$$

Eiji Saitoh et al. Nature 432, 203(2004)

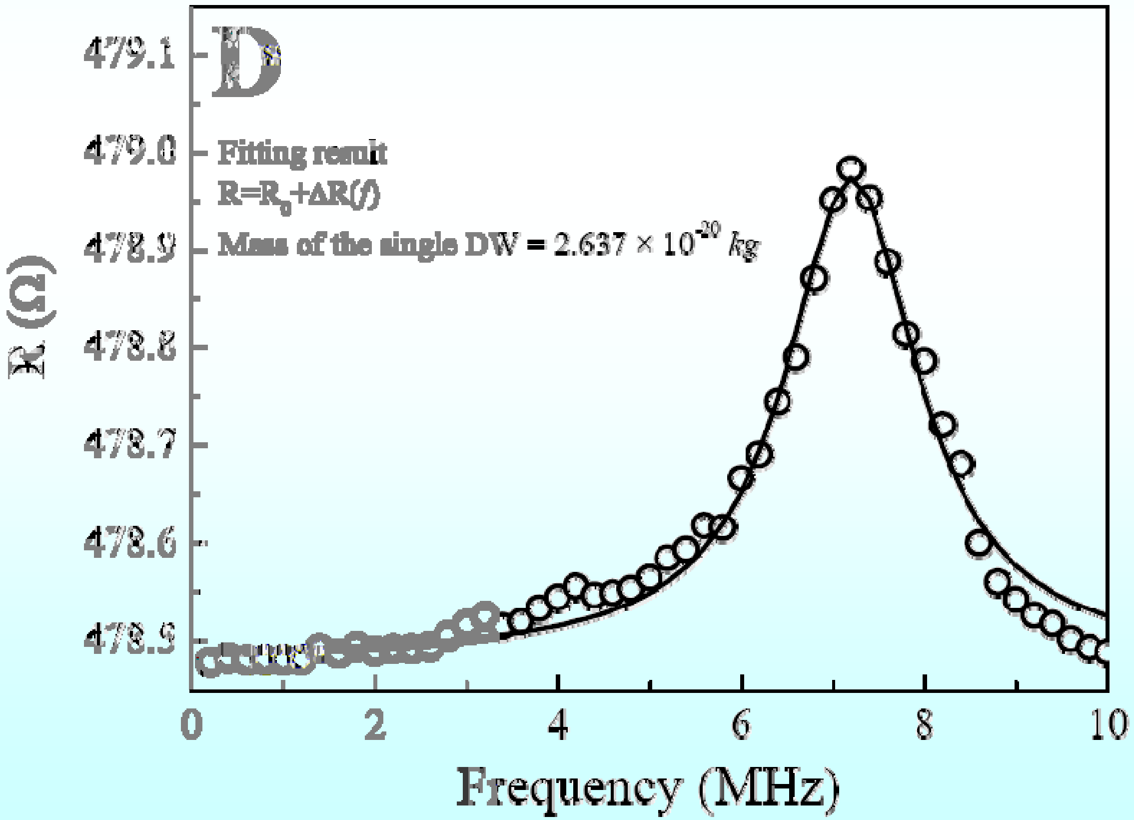

Nowaday Spintronic logic devices

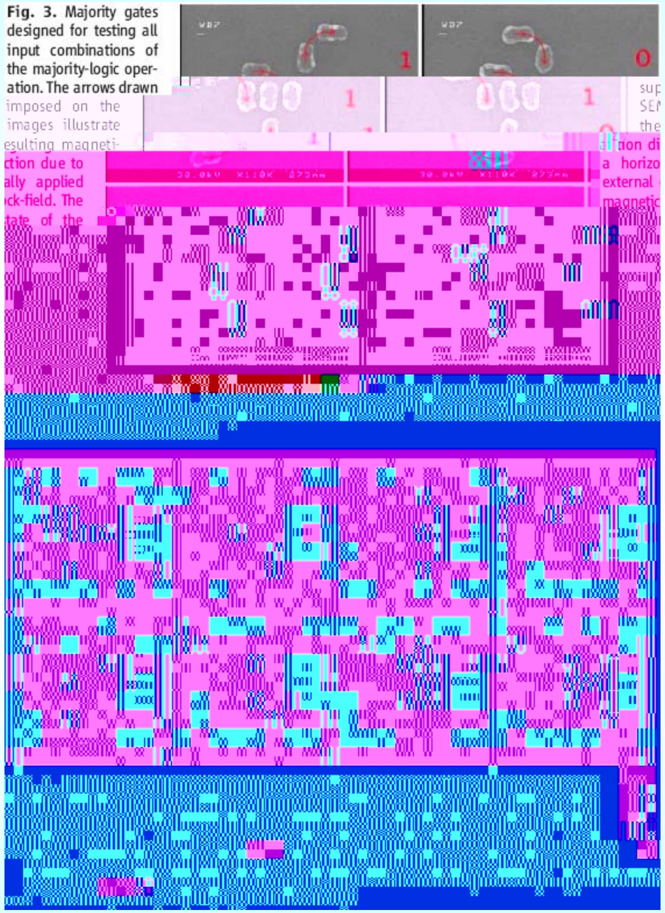

A.Imre et al. Science 311,205

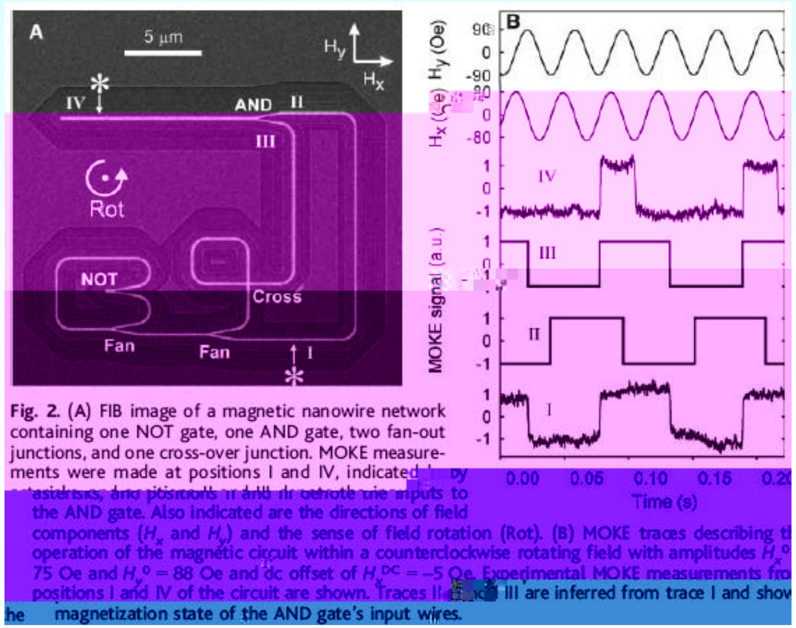

Fig. 2. (A) FIB image of a magnetic nanowire network containing one NOT gate, one AND gate, two fan-out junctions, and one cross-over junction. MOKE measurements were made at positions I and IV, indicated by asterisks, and positions II and III denote the inputs to the AND gate. Also indicated are the directions of field components (H_x and H_y) and the sense of field rotation (Rot). (B) MOKE traces describing the operation of the magnetic circuit within a counterclockwise rotating field with amplitudes H_x^0 = 75 Oe and H_y^0 = 88 Oe and dc offset of H_x^{DC} = –5 Oe. Experimental MOKE measurements from positions I and IV of the circuit are shown. Traces II and III are inferred from trace I and show the magnetization state of the AND gate's input wires.

Cowburn et al. Science 309,1688

Driven by Magnetic field

detected by MFM or MOKE

Not compatible for CMOS circuit

NOT gate circuit

Equivalence circuit

I_{DD}

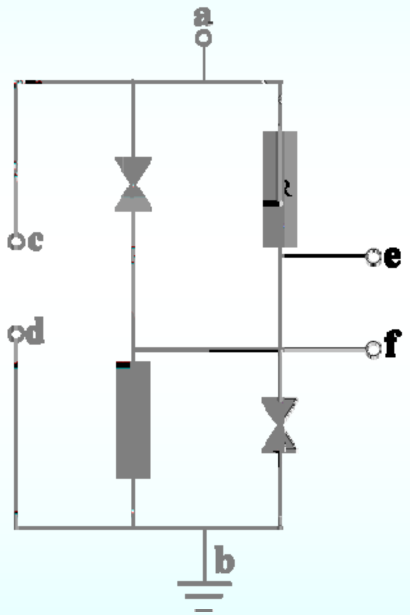

input

output

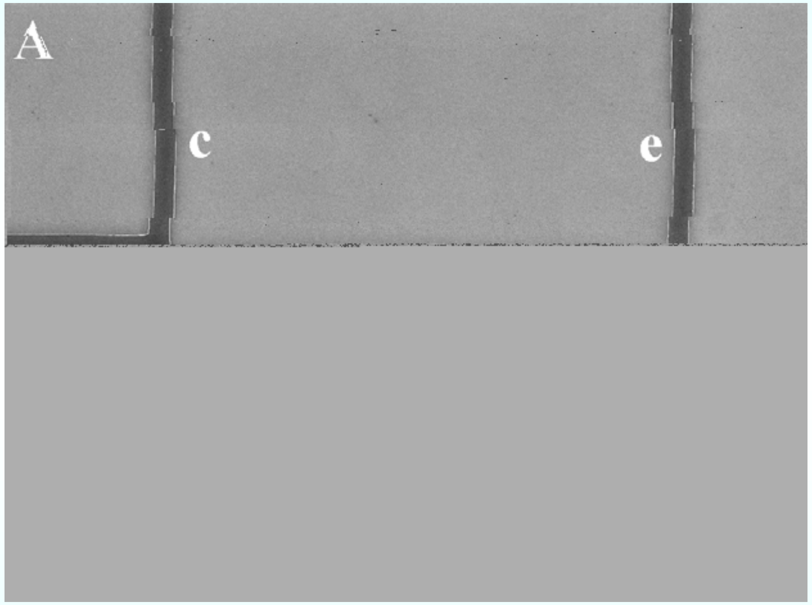

I_{DD} ≈ <critical value

$R = R_{\text{low resistance}}$

Gu et al. Nature Nanotechnology 3 2008 97

NOT gate circuit

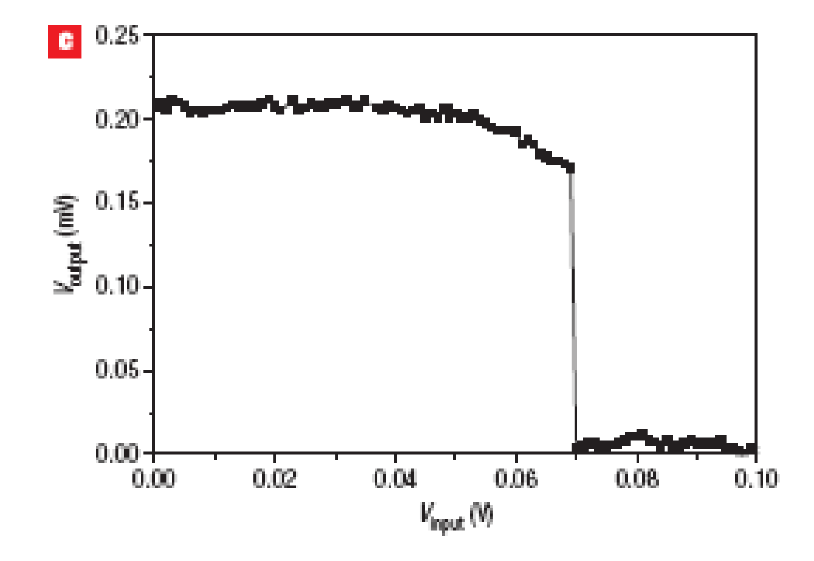

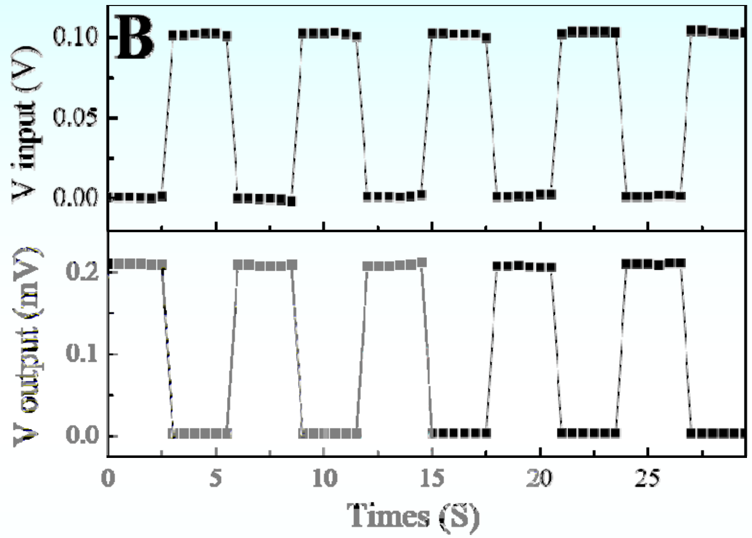

• the intrinsic oscillation frequency of a 50-nm nanocontact is 7.5 ± 0.1 MHz, thus the NOT circuit made from two 50-nm nanocontacts could reach the maximum logic computing speed of 7.5 ± 0.1 MHz.

• the power dissipation could be estimated using the relation $P=VI=1.2\times10^{-4}$ W (where $V=0.24$ V and $I=5.1\times10^{-4}$ A, obtained from experimental data), which is very low compared with that of a Si circuit.

NOT gate circuit

- **work at room temperature without the use of an applied magnetic field**

- **the high carrier densities made possible by the use of metals rather than semiconductors**

- **the electrical controls should make it relatively straightforward to communicate with standard CMOS circuitry**

- **the relative simplicity of the circuits should also make it possible to scale the circuits to smaller sizes.**